AMERICAN SOCIETY FOR MICROBIOLOGY | Applied and Environmental Microbiology®

ENVIRONMENTAL MICROBIOLOGY

Cross Talk between Calcium and Reactive Oxygen Species Regulates Hyphal Branching and Ganoderic Acid Biosynthesis in *Ganoderma lucidum* under Copper Stress

Tan Gao,[a] Liang Shi,[a] Tianjun Zhang,[a] Ang Ren,[a] Ailiang Jiang,[a] Hanshou Yu,[a] Mingwen Zhao[a]

[a]Department of Microbiology, College of Life Sciences, Nanjing Agricultural University; Key Laboratory of Agricultural Environmental Microbiology, Ministry of Agriculture, Nanjing, Jiangsu, People's Republic of China

ABSTRACT *Ganoderma lucidum* is among the best known medicinal basidiomycetes due to its production of many pharmacologically active compounds. To study the regulatory networks involved in its growth and development, we analyzed the relationship between reactive oxygen species (ROS) and Ca^{2+} signaling in the regulation of hyphal branching and ganoderic acid (GA) biosynthesis after Cu^{2+} treatment. Our results revealed that Cu^{2+} treatment decreased the distance between hyphal branches and increased the GA content and the intracellular levels of ROS and Ca^{2+}. Further research revealed that the Cu^{2+}-induced changes in hyphal branch distance, GA content, and cytosolic Ca^{2+} level were dependent on increases in cytosolic ROS. Our results also showed that increased cytosolic Ca^{2+} could reduce cytosolic ROS by activating antioxidases and modulating Cu^{2+} accumulation, resulting in feedback to adjust hyphal growth and GA biosynthesis. These results indicated that cytosolic ROS and Ca^{2+} levels exert important cross talk in the regulation of hyphal growth and GA biosynthesis induced by Cu^{2+}. Taken together, our results provide a reference for analyzing the interactions among different signal transduction pathways with regard to the regulation of growth and development in other filamentous fungi.

IMPORTANCE *Ganoderma lucidum*, which is known as an important medicinal basidiomycete, is gradually becoming a model organism for studying environmental regulation and metabolism. In this study, we analyzed the relationship between reactive oxygen species (ROS) and Ca^{2+} signaling in the regulation of hyphal branching and ganoderic acid (GA) biosynthesis under Cu^{2+} stress. The results revealed that the Cu^{2+}-induced changes in the hyphal branch distance, GA content, and cytosolic Ca^{2+} level were dependent on increases in cytosolic ROS. Furthermore, the results indicated that increased cytosolic Ca^{2+} could reduce cytosolic ROS levels by activating antioxidases and modulating Cu^{2+} accumulation. The results in this paper indicate that there was important cross talk between cytosolic ROS and Ca^{2+} levels in the regulation of hyphal growth and GA biosynthesis induced by Cu^{2+}.

KEYWORDS *Ganoderma lucidum*, copper stress, reactive oxygen species, calcium, ganoderic acids, hyphal branching

Ganoderma lucidum is one of the best known medicinal basidiomycetes in China and Southeast Asia because it contains many pharmacologically active compounds. Ganoderic acids (GAs), which are among the important active compounds isolated from *G. lucidum*, show remarkable pharmacological activity and a variety of therapeutic effects on a number of human diseases; GAs are also hallmarks of secondary metabolism in *G. lucidum* (1). Current research on *G. lucidum* largely focuses on separating the active components and attempting to understand the underlying mechanisms that regulate the synthesis of secondary metabolites (2). The mechanisms

Received 21 February 2018 **Accepted** 16 April 2018

Accepted manuscript posted online 20 April 2018

Citation Gao T, Shi L, Zhang T, Ren A, Jiang A, Yu H, Zhao M. 2018. Cross talk between calcium and reactive oxygen species regulates hyphal branching and ganoderic acid biosynthesis in *Ganoderma lucidum* under copper stress. Appl Environ Microbiol 84:e00438-18. https://doi.org/10.1128/AEM.00438-18.

Editor Haruyuki Atomi, Kyoto University

Address correspondence to Mingwen Zhao, mwzhao@njau.edu.cn.

T.G. and L.S. contributed equally to this work.

of biosynthetic regulation are difficult to study due to the complexity of the active compounds in *G. lucidum* and the specific developmental patterns of filamentous fungi. However, the recent publication of the *G. lucidum* genome sequence (3) and the development of molecular genetic tools (4, 5) have contributed to further analyses. Based on this research progress, *G. lucidum* could become a model system for studying the complex growth patterns and regulation of secondary metabolic pathways in filamentous fungi.

Research on the regulation of GA biosynthesis has mainly employed the classical method of optimizing and controlling the fermentation process (6–8). Involvement of the following exogenous substances in GA biosynthesis has also been reported: aspirin (9), phenobarbital (10), acetate (11), and methyl jasmonate (MeJA) (12). Additional studies have found that many signaling pathways may participate in the regulation of GA biosynthesis in *G. lucidum*, including those involving ROS and Ca^{2+} (13, 14).

Both ROS and Ca^{2+} are important intracellular messengers and are involved in regulating the biosynthesis of secondary metabolites. In higher plants, ROS signaling is involved in proline metabolism and plays a vital role in senescence (15). Aflatoxin production in *Aspergillus parasiticus* was inhibited by treatment with Ca^{2+} channel blockers, which suggests the importance of Ca^{2+} in the production of these secondary metabolites (16). In *G. lucidum*, NADPH oxidases (Nox), which are the main source of ROS, were found to positively regulate GA biosynthesis and hyphal growth (17). MeJA has been reported to induce GA biosynthesis and generate a Nox-dependent ROS burst, and the GA biosynthesis induced by MeJA treatment was abolished by ROS scavengers or in Nox-silenced mutants. These findings suggest that ROS play an important role in the biosynthetic regulation elicited by MeJA treatment (13). In addition, You et al. reported that aspirin was able to induce GA biosynthesis via ROS accumulation and cell apoptosis in *G. lucidum*, indicating that ROS may be involved in regulating GA biosynthesis (9). Cellular Ca^{2+}, a ubiquitous second messenger, is also involved in the biosynthetic regulation of GAs in *G. lucidum*. Sequence analysis revealed that the promoters of key GA biosynthetic genes (*hmgr*, *osc*, and *sqs*) contain a putative calcineurin-responsive zinc finger transcription factor (Crz)-binding element and that the gene expression of cytosolic Ca^{2+} sensors was upregulated with Ca^{2+} addition. Overall, this evidence suggests that Ca^{2+} signal transduction has a substantial effect on GA biosynthesis (18). Additionally, there are reports that exogenous H_2O_2 treatment activates Ca^{2+} channels that induce Ca^{2+} influx and elevate cytosolic Ca^{2+} to regulate GA biosynthesis, a process that could be inhibited with a Ca^{2+} channel blocker (17). The effects of glutathione peroxidase (GPx) on GA biosynthesis via ROS are also regulated by cytosolic Ca^{2+} content and are associated with Ca^{2+} pathway-related gene expression (14). Thus, the research to date indicates that both ROS and Ca^{2+} signaling pathways participate in the regulation of GA biosynthesis and that some interaction between ROS and Ca^{2+} signaling may be observed in *G. lucidum*. However, because the exact mechanism of ROS- and Ca^{2+}-regulated GA biosynthesis remains unclear, studies aimed at a comprehensive understanding of the relationship between signaling and GA biosynthesis are worth pursuing.

As a third key modulator after calcium and zinc, copper can induce changes in the intracellular ROS and Ca^{2+} contents (19) and affect various physiological and biochemical responses (20). Copper has also reportedly been used as an inducer to increase the GA content during submerged fermentation (21). Copper, which is an exogenous environmental factor, could be optimal for resolving the roles of ROS and Ca^{2+} in the regulation of development and metabolism in *G. lucidum*. We examined the potential cross talk between cytosolic Ca^{2+} and ROS levels under copper stress and analyzed their roles in copper-induced changes in hyphal branching and GA biosynthesis in *G. lucidum*. Our results indicate that a burst of ROS under copper stress is important for regulating hyphal branching and GA biosynthesis. Based on the increase in cytosolic Ca^{2+} content under copper stress, our work suggests that such an increase in cytosolic Ca^{2+} may affect ROS levels by regulating antioxidase activity to modulate hyphal growth and GA biosynthesis. In addition, our results also indicated that increased

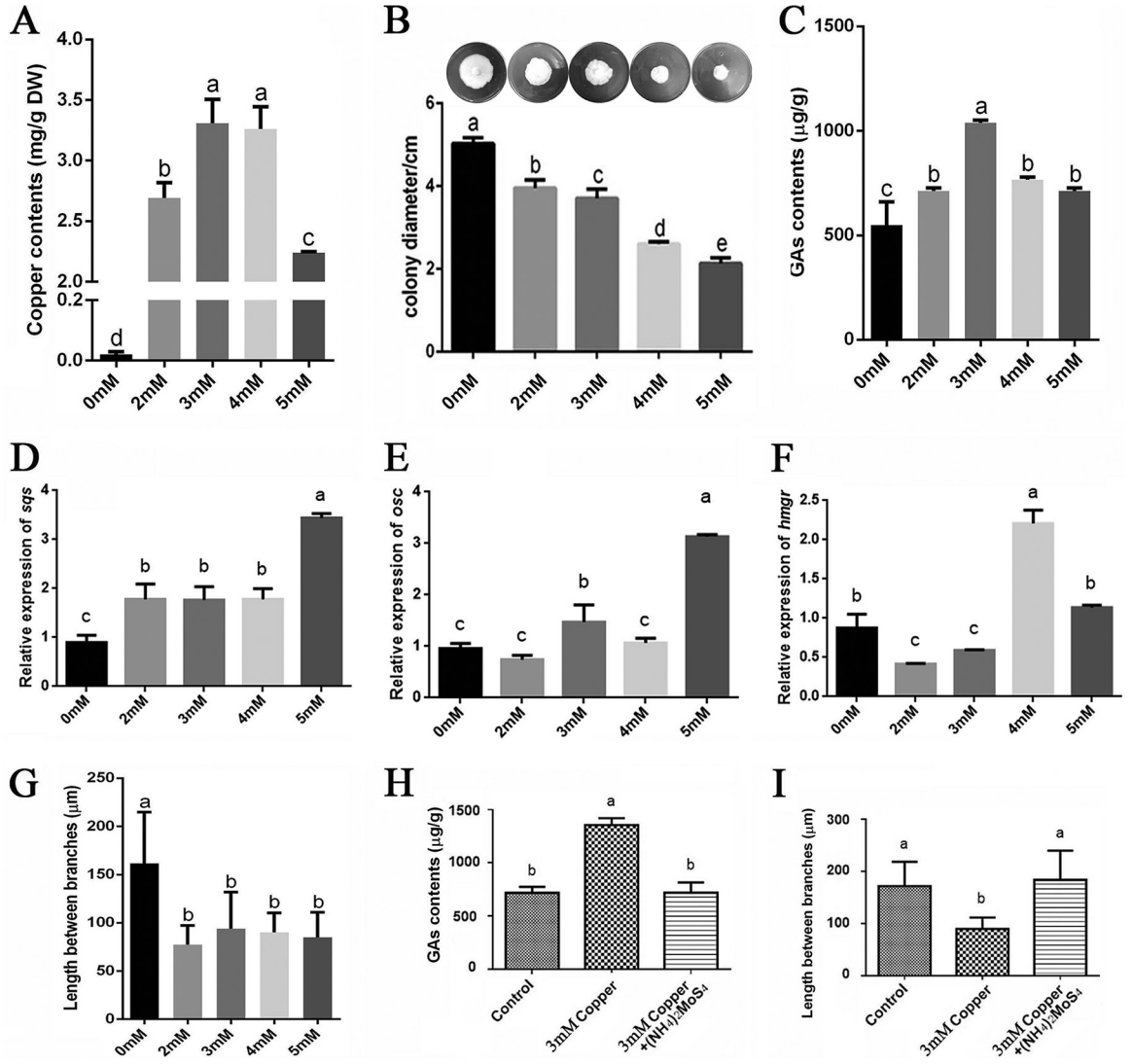

FIG 1 Copper stress regulates the accumulation of intracellular copper, hyphal branching, and GA biosynthesis in *G. lucidum*. (A) The *G. lucidum* WT strain was cultured in liquid CYM with shaking at 28°C. On the 4th day, various concentrations of copper were added. On the 7th day, the samples were analyzed. The levels of intracellular copper accumulation were measured by microwave digestion generation atomic fluorescence spectrometry and ICP-OES. (B) Effect of various copper concentrations on hyphal growth and colony diameter. (C) A UPLC method was used to measure the GA content in *G. lucidum* cultures treated with various concentrations of copper. (D to F) Measurements of the relative expression of genes that encode key enzymes in the GA biosynthetic pathway under various concentrations of copper: *hmgr* (encoding 3-hydroxy-3-methylglutaryl coenzyme A reductase), *sqs* (encoding squalene synthase), and *osc* (encoding lanosterol synthase). (G) The *G. lucidum* WT strain was cultured on CYM plates for 5 days with various concentrations of copper. Aerial hyphae were removed from actively growing colonies, suspended in 2.5 $\mu g \cdot ml^{-1}$ Fluorescent brightener 28, and observed using a Nikon Eclipse Ti-S microscope with UV light. The distance between two hyphal branches was measured in the fluorescence image. (H) Changes in the GA contents in copper-stressed cultures in the presence of a copper chelator. (I) Changes in the hyphal branch distance in *G. lucidum* in copper-stressed cultures in the presence of a copper chelator. All values are the mean ± standard deviation (SD) of the results from three independent experiments. Within each set of experiments, different letters indicate significant differences between the lines ($P < 0.05$, according to a multiple-comparison one-way ANOVA).

cytosolic Ca^{2+} modulates the accumulation of intracellular copper. Our research offers a new approach to understanding the regulatory mechanisms that underlie the biochemical/physiological responses to other environmental factors in *G. lucidum*.

RESULTS

Copper stress regulates GA biosynthesis and hyphal branching in *G. lucidum*. To precisely determine the effect of copper on GA biosynthesis in *G. lucidum*, we first measured the copper content in *G. lucidum* mycelia after treatment with various concentrations of copper. As illustrated in Fig. 1A, the copper content in *G. lucidum*

mycelia without copper treatment was 0.02 mg/g (dry weight [DW]). This value was significantly increased by the various treatments. The copper content was increased to 2.69 mg/g (DW) with 2 mM copper treatment, 3.31 mg/g (DW) with 3 mM copper treatment, 3.26 mg/g (DW) with 4 mM copper treatment, and 2.24 mg/g (DW) with 5 mM copper treatment (Fig. 1A). These results indicate that exogenous copper could significantly augment the endogenous copper content. Additionally, the effects on hyphal growth of different copper concentrations were also investigated (Fig. 1B). The results demonstrated that growth was significantly inhibited by the treatments with increasing concentrations of copper, especially in the groups treated with 4 or 5 mM copper.

We then measured the GA content after treatment with the various concentrations of copper (Fig. 1C). Among the tested concentrations, the level of GAs exhibited a maximum 91% increase relative to the control at 3 mM copper. In addition, real-time PCR (RT-PCR) was used to analyze the effects of copper stress on the gene expression of key enzymes in the GA biosynthetic pathway, including *sqs* (encoding squalene synthase), *osc* (encoding lanosterol synthase), and *hmgr* (encoding 3-hydroxy-3-methylglutaryl coenzyme A reductase). As shown in Fig. 1D to F, these three genes were generally upregulated under copper stress. The expression levels of *sqs* and *osc* were significantly increased in the 3 mM copper-treated sample. The expression of *hmgr* was significantly increased in the 4 mM copper-treated sample but decreased in the 3 mM copper-treated sample. This result provides support for the concept that copper induces GA biosynthesis. This result also shows that the expression of the *sqs* and *osc* genes was most highly upregulated in the samples treated with 5 mM copper (Fig. 1D and E), although the copper content in *G. lucidum* mycelia was significantly lower in those treated with 5 mM copper (Fig. 1A). The discrepancy between the transcription and GA content data could be explained by differences in the stability of mRNA. The activity of the enzymes could also affect GA biosynthesis.

To explore whether GA biosynthesis is a global response to metal stress or is specific to copper stress alone, we analyzed the effect of two other metals, iron and cadmium, on GA biosynthesis. The results are shown in Fig. S1 in the supplemental material and indicate that GA content could be increased by 3 mM Cd^{2+} but could not be increased by 3 mM Fe^{3+}.

Hyphal branching is an important developmental behavior in filamentous fungi and is closely related to growth and nutrient absorption. To investigate the effect of copper stress on growth in *G. lucidum*, the distance between pairs of branches was measured in the wild-type (WT) strain cultured on solid complete yeast medium (CYM) with various concentrations of copper. Statistically, the data revealed that the various concentrations of copper could decrease the hyphal branch distances in the WT strain compared with no treatment (Fig. 1G). The mean hyphal branch distance was significantly reduced from 160 μm to approximately 90 μm under the various levels of copper stress. Furthermore, a copper-specific chelator [$(NH_4)_2MoS_4$] was used to show that a reduction in Cu^{2+} concentration could reduce GA production and increase the hyphal branch distance (Fig. 1H and I).

The above-described results demonstrated that copper stress could reduce the hyphal branch distance and enhance GA biosynthesis in *G. lucidum*.

Copper stress increases the concentrations of ROS and Ca^{2+}. The levels of ROS and Ca^{2+} in mycelia exposed to copper were also investigated by dichlorodihydrofluorescein diacetate (DCFH-DA) and Fluo-3 AM staining. As indicated in Fig. 2A and C, increases in the green fluorescence intensity were observed under copper stress compared with the control, which demonstrated that copper stress induced an increase in the level of cytosolic ROS. The production of ROS was markedly increased by 53% with 2 mM copper and 104% with 3 mM copper, reached a maximum of 168% with 4 mM copper, and decreased slightly to 163% with 5 mM copper (Fig. 2A and C). In addition, the level of cytosolic Ca^{2+} was also significantly enhanced by the addition of various concentrations of copper (Fig. 2B and D), increasing by 64% with 2 mM and

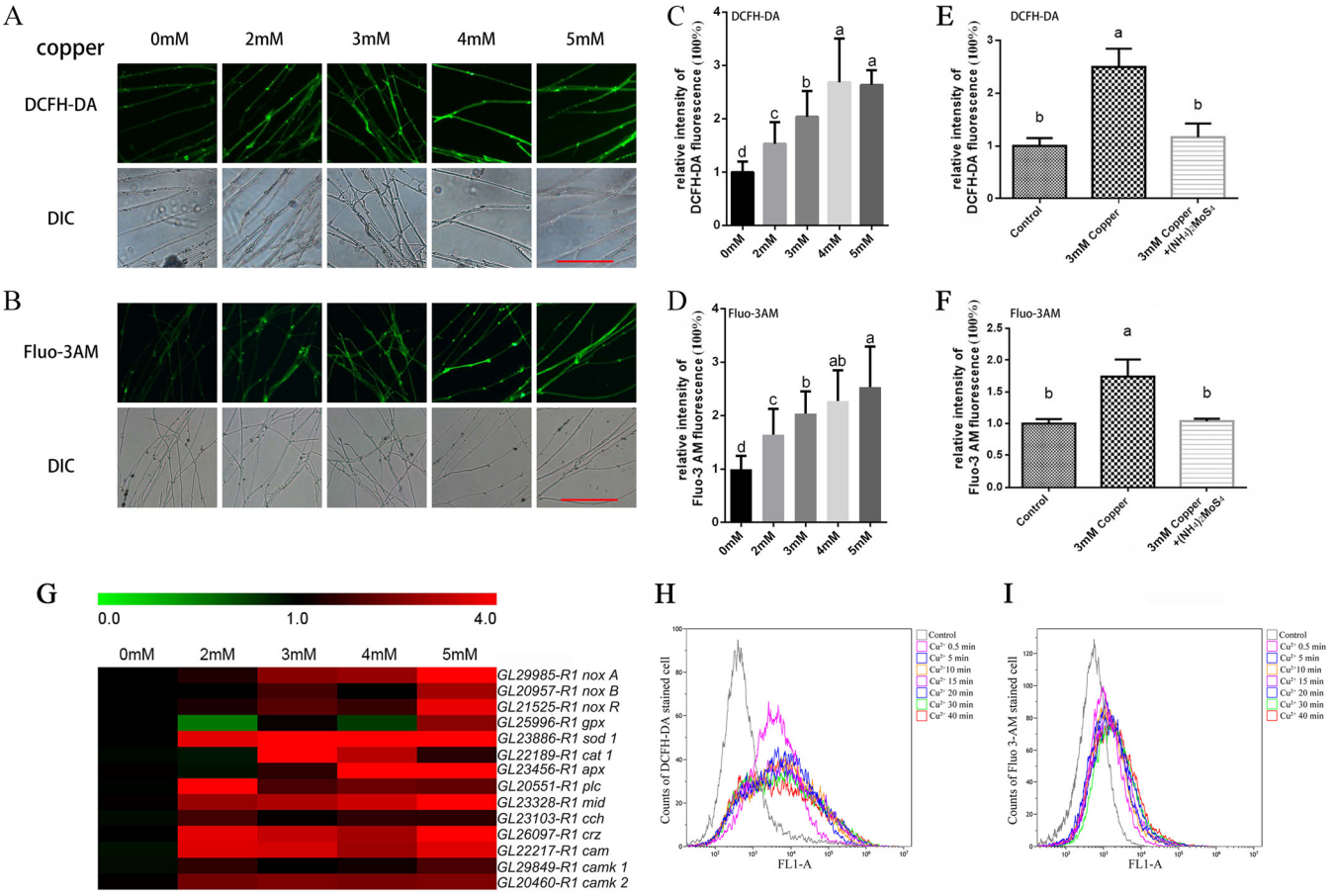

FIG 2 Copper stress increases the concentration of ROS and Ca^{2+} and the expression of related genes. The *G. lucidum* WT strain was cultured on CYM plates for 5 days with various concentrations of copper. Aerial hyphae were removed from actively growing colonies, suspended in either the fluorescent dye DCFH-DA to measure the cytosolic ROS (A) or Fluo-3AM to measure the free cytosolic Ca^{2+} (B) for 30 min at 37°C. The hyphae were washed three times with PBS to remove excess fluorophore. The green fluorescence of the DCF- and Fluo-3-labeled cells was visualized by confocal laser scanning microscopy (CLSM), with the green fluorescence intensity representing the levels of cytosolic ROS and Ca^{2+}. DIC, differential interference contrast. Scale bar = 100 μm. (C and D) Changes in the cytosolic ROS and Ca^{2+} fluorescence ratios in copper-stressed *G. lucidum*. The *y* axis represents the fluorescence ratio measured by CLSM, and the *x* axis represents the various concentrations of copper. Within each set of experiments, different letters indicate significant differences between the lines ($P < 0.05$, according to a multiple-comparison one-way ANOVA). (E) Changes in the cytosolic ROS fluorescence ratio in copper-stressed cultures in the presence of a copper chelator. (F) Changes in the cytosolic Ca^{2+} fluorescence ratio in copper-stressed cultures in the presence of a copper chelator. (G) The WT strain was cultured in liquid CYM with shaking at 28°C. On the 4th day, various concentrations of copper were added. On the 7th day, the samples were analyzed. The expression levels of certain ROS and Ca^{2+} signaling-related genes were measured after the hyphae were treated for 3 days with various concentrations of copper. The relevant genes were measured using real-time PCR with the 18S rRNA gene as a reference gene, and the results are presented as a heatmap generated using GeneSpring GX 7.3.1 software (Agilent Technologies). The relative expression is shown as a mean value from 0.0 to 4.0 in green to red. *noxA* is GL29985-R1, *noxB* is GL20957-R1, *noxR* is GL21525-R1, *gpx* is GL25995-R1, *sod1* is GL23886-R1, *cat1* is GL22189-R1, *apx* is GL23456-R1, *plc* is GL20551-R1, *mid* is GL23328-R1, *cch* is GL23103-R1, *crz* is GL26097-R1, *cam* is GL22217-R1, *camk1* is GL29849-R1, and *camk2* is GL20460-R1. The values are the mean ± SD of the results from three independent experiments. (H and I) Dynamic detection by flow cytometry of ROS and Ca^{2+} in *G. lucidum* at early times during the copper treatment. The *y* axis represents the count of stained cells, and the *x* axis, shown as FL1-A, represents the DCFH-DA (H) and Fluo 3-AM (I) fluorescence intensity.

103% with 3 mM and reaching maxima of 127% with 4 mM and 153% with 5 mM. These results indicate that copper stress induced increases in the levels of both cytosolic ROS and Ca^{2+}. Furthermore, a copper-specific chelator [$(NH_4)_2MoS_4$] was used to show that a reduction in Cu^{2+} concentration could reduce ROS and Ca^{2+} levels (Fig. 2E and F).

The above-described results demonstrated that increases in the ROS and Ca^{2+} contents were determined in response to copper stress. To further verify the effect of copper on the ROS and Ca^{2+} signaling pathway, an RT-PCR assay was carried out to analyze the transcription levels of certain ROS and Ca^{2+} signaling-related genes, including NADPH oxidase family genes (*noxA*, *noxB*, and *noxR*), antioxidant enzyme genes (*gpx*, *sod*, *cat*, and *apx*), Ca^{2+} channel-related genes (*plc*, *mid*, and *cch*), and Ca^{2+} signaling pathway genes (*crz*, *cam*, *camk1*, and *camk2*), after treatment with various concentrations of copper (Fig. 2G). The primers used to detect transcriptional changes

TABLE 1 Oligonucleotide primers used

Primer	Sequence (5′ to 3′)	Detection
SqsRT-F	CTGCTTATTCTACCTGGTGCTACG	*sqs* gene expression
SqsRT-R	GGCTTCACGGCGAGTTTGT	
OscRT-F	AGGGAGAACCCGAAGCATT	*osc* gene expression
OscRT-R	CGTCCACAGCGTCGCATAAC	
HmgrRT-F	GTCATCCTCCTATGCCAAAC	*hmgr* gene expression
HmgrRT-R	GGGCGTAGTCGTAGTCCTTC	
NoxaRT-F	CGTAGAGTTCTTCTGGGTTTGC	*noxA* gene expression
NoxaRT-R	CTGCGTGAGGTAGATGTTGATA	
NoxbRT-F	TTCGCGTCGATCCTCAAGT	*noxB* gene expression
NoxbRT-R	GTTCTGCGTGTCCTGCTCC	
NoxrRT-F	GCAGCTATGGAGGCAGCATG	*noxR* gene expression
NoxrRT-R	TCGCGGTAGTACAGCTTCACG	
GPxRT-F	ATGTCCGACGCAGGATTCTACT	*gpx* gene expression
GPxRT-R	GGAAGCCGAGAATGACGAAG	
CAT1RT-F	TACGGTATTCAGCTCTTGT	Catalase 1 expression
CAT1RT-R	TGTTGTAACGGAACTTCTC	
SOD1RT-F	ATCGCCGTCTTCGTCGTTT	Superoxide dismutase 1 gene expression
SOD1RT-R	GTGACTGGTGCGGTAGGGA	
APXRT-F	TTTTCGGTGCCCTTGGTGC	Ascorbate peroxidase gene expression
APXRT-R	GTAGTTCTTATCAGCCGCCT	
PlcRT-F	CAACTTTGACGACGTAGAGC	Phospholipase C gene expression
PlcRT-R	GGCGTGCCTTGAGGGACTT	
MidRT-F	AACTTGTCCTTGCCATCACC	*mid* expression
MidRT-R	CCAGCCATCCGTATTCTTC	
CchRT-F	GCTGGTGCTGGGTAGGA	*cch* expression
CchRT-R	TCCAGTCAGGCAAATAGG	
CrzRT-F	ACGCCCCTTCCTATGCGAGTG	Calcineurin-responsive zinc finger transcription factor expression
CrzRT-R	AGGAAACGGCGTCAGTAGC	
CamRT-F	CCCCGAGTTCCTGACGATG	Protein that undergoes conformational change upon binding to Ca^{2+} expression
CamRT-R	AGCTTCTCGCCGAGGTTGG	
CamK1RT-F	GTCGATATGTGGTCAACAGGGATT	*camk*1 gene expression
CamK1RT-R	ACGGTCGGTGGGAAGTCAGC	
CamK2RT-F	GAAGTTCCACCTCTTGACGG	*camk*2 gene expression
CamK2RT-R	TCACCACGGATGATAGCC	
18SRT-F	TATCGAGTTCTGACTGGGTTGT	Expression of the 18S rRNA gene as a reference gene
18SRT-R	ATCCGTTGCTGAAAGTTGTAT	

in these genes are listed in Table 1 (17). As shown in Fig. 2G, similar to the changes in the contents of cytosolic ROS and Ca^{2+}, the expression of these genes was significantly upregulated in the samples treated with copper.

To detect earlier changes in the ROS and Ca^{2+} contents during the treatment with copper, flow cytometry was employed to continuously analyze the ROS and Ca^{2+} dynamics from the beginning of the 3 mM copper treatment. As shown in Fig. 2H and I, the 3 mM copper treatment significantly increased the proportion of highly fluorescent cells stained with the ROS and Ca^{2+} dyes after treatment with copper for only 30 s. During extended copper treatment, the proportion of fluorescent cells remained high. These results suggested that copper stress could increase the concentrations of ROS and Ca^{2+} and activate the expression of the above-mentioned signaling-related genes in *G. lucidum*.

Copper stress-regulated GA biosynthesis and hyphal branching are dependent on ROS overproduction. The results presented above show that the ROS contents were increased by treatment with copper. To validate the role of copper stress-induced ROS on the regulation of hyphal branching and GA biosynthesis, several different inhibitors of ROS generation were applied, including dibenziodolium chloride (DPI; an NADPH oxidase inhibitor), rotenone (Rot; a mitochondrial complex I inhibitor), and antimycin A (AA; a mitochondrial complex III inhibitor). For each inhibitor (DPI, Rot, and AA), the effects of two concentrations were examined. Because the same trend was observed for the two concentrations, the data for the group treated with only one concentration of each inhibitor are presented. The results showed that the overproduction of ROS in the mycelia was effectively inhibited to various degrees by DPI, Rot,

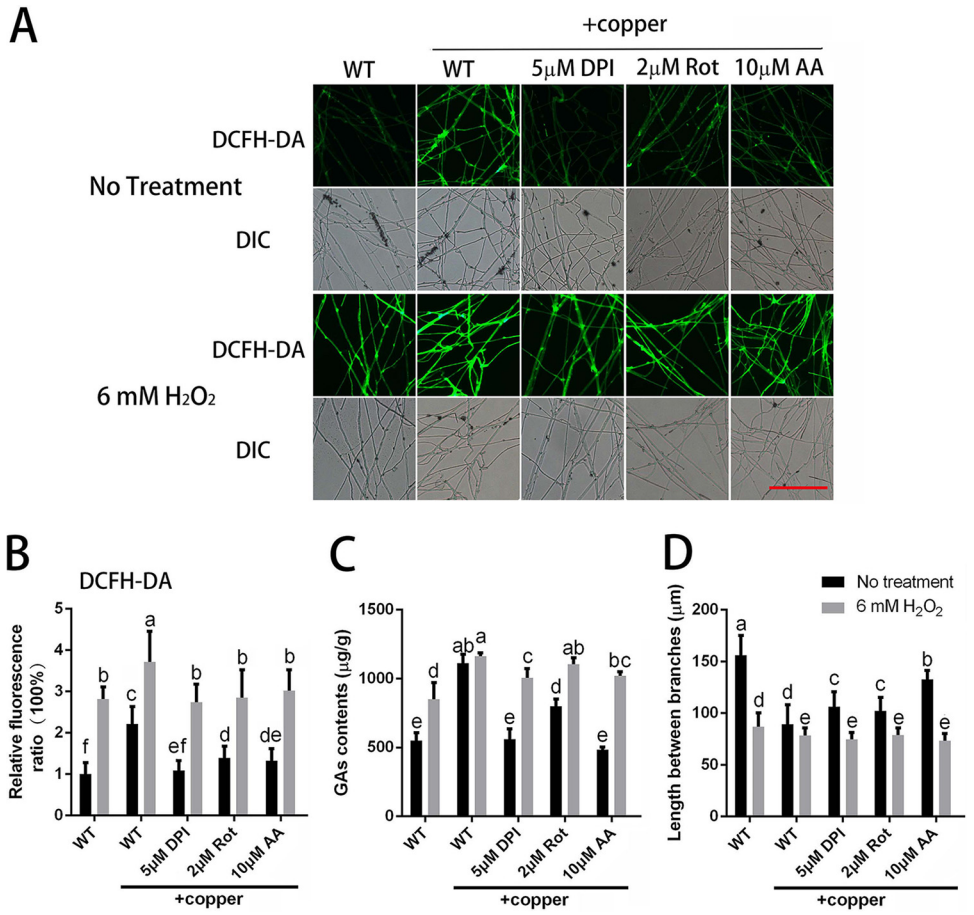

FIG 3 Copper stress-regulated hyphal branching and GA biosynthesis are dependent on ROS accumulation. (A) Changes in ROS levels in *G. lucidum* were determined by using DCFH-DA staining after treatment with ROS-related inhibitor, H_2O_2, or 3 mM copper. Scale bar = 100 μm. (B) Changes in the ROS fluorescence ratio in the hyphal regions of *G. lucidum* after treatment with the ROS-related inhibitor, H_2O_2, or 3 mM copper. The *y* axis represents the ROS fluorescence ratio measured by CLSM, and the *x* axis represents the various treatments. (C) Measurement of the GA content in *G. lucidum* after treatment with the ROS-related inhibitor, H_2O_2, or 3 mM copper. (D) Measurement of the hyphal branch distance in *G. lucidum* after treatment with the ROS-related inhibitor, H_2O_2, or 3 mM copper. DPI was used as an NADPH oxidase inhibitor, Rot (rotenone) was used as a mitochondrial complex I inhibitor, and AA (antimycin A) was used as a mitochondrial complex III inhibitor. The values are the mean ± SD of the results from three independent experiments. Within each set of experiments, different letters indicate significant differences between the lines ($P < 0.05$, according to a multiple-comparison one-way ANOVA).

and AA (Fig. 3A and B). Differences in the fold changes in ROS induced by exposure to copper were also observed between the wild-type (WT) and DPI-, Rot-, or AA-treated *G. lucidum* mycelia (Fig. S2A). The results demonstrated that the copper-induced fold changes of ROS in the DPI-, Rot-, or AA-treated cultures became closer to 1, which indicated that treatment with DPI-, Rot-, or AA could reduce the effect caused by copper. These results indicated that ROS was generated by complex sources, such as NADPH oxidase (NOX) and mitochondria, and that these sources might interact with each other. These results indicated that various concentrations of different ROS inhibitors could significantly inhibit the increase in ROS content induced by copper stress. These results suggested that the upregulation of ROS levels stimulated by 3 mM copper treatment could be prevented by ROS inhibitors.

To validate the effects of ROS on GA biosynthesis and hyphal branching, we assessed the changes in hyphal branching and GA biosynthesis observed when ROS production inhibitors were applied concurrently with copper stress. As shown in Fig. 3C, the increase in the GA content induced by 3 mM copper stress could be effectively blocked by treatment with DPI, Rot, or AA. The copper-induced changes in the GAs

between WT and DPI-, Rot-, or AA-treated *G. lucidum* mycelia were also examined (Fig. S2B). The results indicated that DPI, Rot, or AA treatment could reduce the effect caused by copper and that NOX and mitochondria might play an important role in copper-induced GA biosynthesis. The RT-PCR results showed that the upregulated expression of GA biosynthesis genes (*sqs*, *osc*, and *hmgr*) induced by 3 mM copper was also significantly inhibited by DPI, Rot, or AA treatment, with trends that were consistent with those of the GA content (Fig. S2D to F). Regarding hyphal branching, the hyphal branch distance was decreased by 43% after the WT strain was treated with 3 mM copper (Fig. 3D). However, compared to the distance in the WT cultures after treatment with 3 mM copper alone, the distance was significantly increased by 14% with 5 μM DPI, by 13% with 2 μM Rot, and by 41% with 10 μM AA. These results indicate that copper stress-induced GA biosynthesis and hyphal branching could be blocked when the copper-induced increase in ROS was inhibited.

To further validate the effect of ROS on GA biosynthesis and hyphal branching, exogenous 6 mM H_2O_2, which had a slight impact on the growth rate compared with that of the control group (Fig. S2F), was added to restore the intracellular ROS content. As shown in Fig. 3A and B, exogenous H_2O_2 treatment notably increased the level of ROS in the WT mycelia, both in the presence or absence of 3 mM copper treatment, and increased the intracellular ROS contents when ROS inhibitors were applied to decrease the overproduction of ROS under copper stress. Changes in the hyphal branching and GA biosynthesis were also assessed after exogenous H_2O_2 treatment. As shown in Fig. 3C, the reduced GA content caused by the ROS inhibitors was significantly increased by the H_2O_2 treatment. RT-PCR also showed that, to various degrees, H_2O_2 treatment induced upregulation of the expression of key GA biosynthetic genes (Fig. S2C to E), and the increased hyphal branch distances were reduced by H_2O_2 treatment (Fig. 3D). These results show that the increase in ROS content induced by 3 mM copper stress could be reduced with inhibitors of ROS generation and that the increase in the GA content and the decrease in hyphal branch distance induced by copper stress could also be reduced. However, these effects were reversed by treatment with exogenous H_2O_2 to restore the intracellular ROS content.

Moreover, to further evaluate the effect of ROS on hyphal branching and GA biosynthesis under copper stress, we utilized Nox-silenced strains and determined the ROS levels after copper treatment (17). As shown in Fig. 4A and B, 3 mM copper stress significantly increased the levels of ROS in the WT and CK strains (empty vector control) compared with WT cultures that were not treated with 3 mM copper. Although copper could increase ROS contents in the Nox-silenced strains compared with the ROS contents in the Nox-silenced strains that were not treated with copper, the ROS contents in the group of Nox-silenced strains treated with copper were lower than those in the copper-treated WT strain. In addition, copper-induced changes in the ROS in the Nox-silenced strains were determined (Fig. S3A). This result demonstrated that copper-induced fold changes in ROS in Nox-silenced strains were significantly increased compared with those in WT and that silencing NOX was detrimental to the ROS balance in cells, which caused the copper stress response to become acute. The GA content was significantly increased by copper stress in the WT and CK strains (Fig. 4C). Compared with the WT strain under copper stress, Nox silencing significantly inhibited the copper-induced increase in the GA content, although copper could increase the GA content in the Nox-silenced strains. In addition, the results shown in Fig. S3B demonstrate that the copper-induced fold changes in the GAs in the Nox-silenced strains were significantly lower than those observed in the WT, which indicated that NOX might play an important role in copper-induced GA biosynthesis. Additionally, the hyphal branch distances in the WT and CK strains under copper stress were significantly reduced compared with those in the WT in the absence of the 3 mM copper treatment (Fig. 4D). However, the distances in Nox-silenced strains under copper stress were partially restored. These results revealed that the increase in ROS content induced by copper stress could be reduced by Nox silencing and that the changes in the GA biosynthesis and hyphal branching induced by copper stress could also be effectively suppressed in

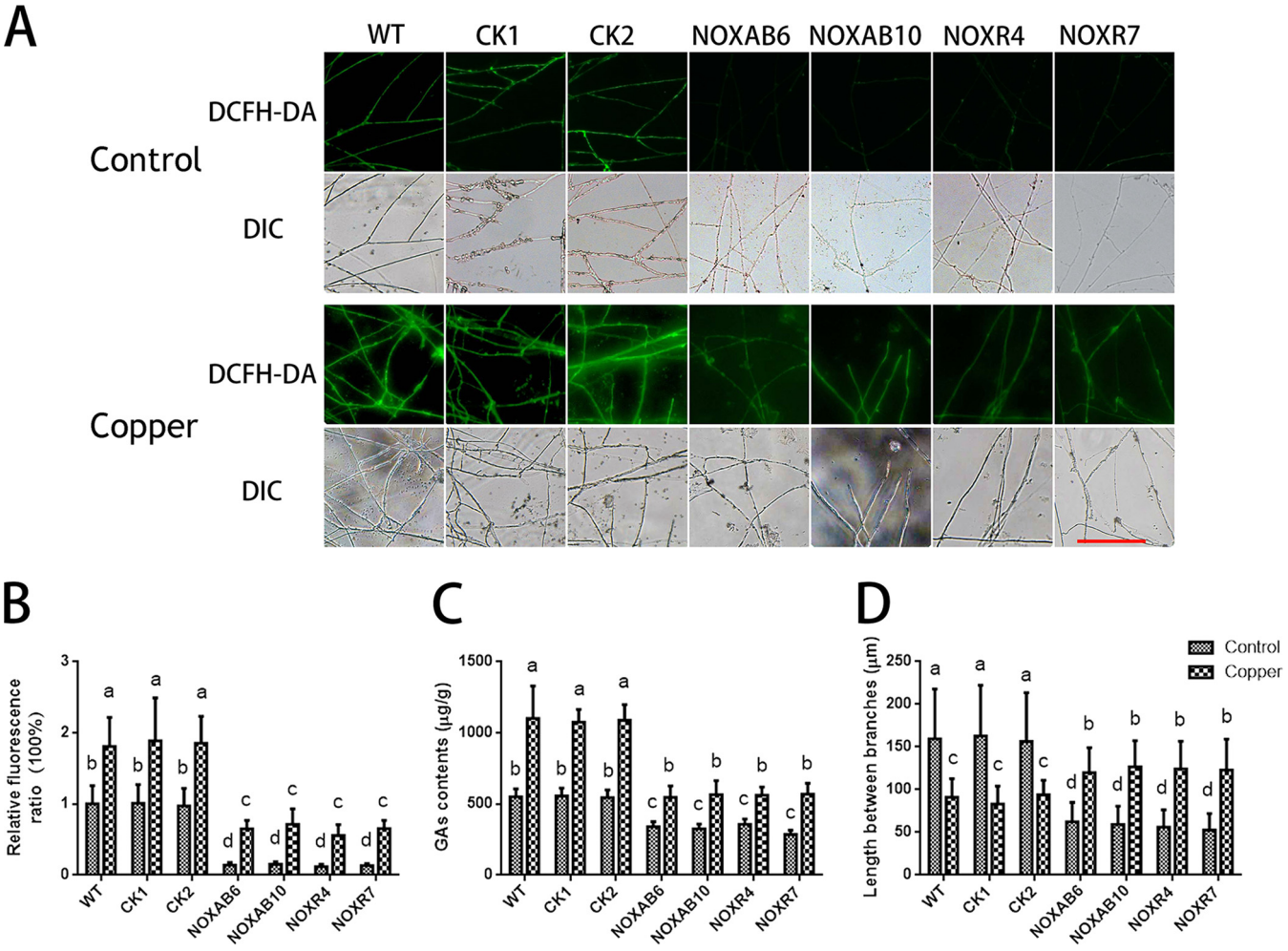

FIG 4 Copper stress-regulated hyphal branching and GA biosynthesis are inhibited in Nox-silenced strains. (A) Changes in ROS levels in Nox-silenced strains were determined by using DCFH-DA staining in cultures treated with or without 3 mM copper. Scale bar = 100 μm. (B) Changes in the ROS fluorescence ratio in the hyphal regions of Nox-silenced strains treated with or without 3 mM copper. The *y* axis represents the ROS fluorescence ratio measured by CLSM, and the *x* axis represents the different strains. (C) Measurement of the GA content in Nox-silenced strains treated with or without 3 mM copper. (D) Measurement of the hyphal branch distance in Nox-silenced strains treated with or without 3 mM copper. WT, wild-type strain; CK1 and CK2, empty vector control strains; NOXAB6 and NOXAB10, NoxAB-silenced strains; NOXR4 and NOXR7, NoxR-silenced strains. The values are the mean ± SD of the results from three independent experiments. Within each set of experiments, different letters indicate significant differences between the lines ($P < 0.05$, according to a multiple-comparison one-way ANOVA).

the Nox-silenced strains. These results were consistent with the results of DPI application.

In general, these results indicated that copper stress-regulated GA biosynthesis and hyphal branching are dependent on ROS overproduction; these findings are consistent with our previous report (13, 17).

Exogenous Ca^{2+} application inhibits the changes in the GA content and hyphal branching induced by copper stress. To investigate the effect of the increased cytosolic Ca^{2+} content induced by 3 mM copper stress on hyphal branching and GA biosynthesis, we used neomycin (Neo; an inhibitor of phospholipase C) to reduce the release of intracellular calcium stores and $LaCl_3$ (a blocker of calcium channels on the plasma membrane) to prevent the influx of external calcium (22). Neo and $LaCl_3$ were each tested at two concentrations. Because the same trend was observed for the two concentrations, the data for the group treated with only one concentration of each agent are shown. As shown in Fig. 5A and B, the increased content of cytosolic Ca^{2+} induced by 3 mM copper stress could be effectively curbed by adding Neo (or $LaCl_3$). These results indicated that the increase in the Ca^{2+} levels induced by 3 mM copper treatment could be attenuated by Neo or $LaCl_3$.

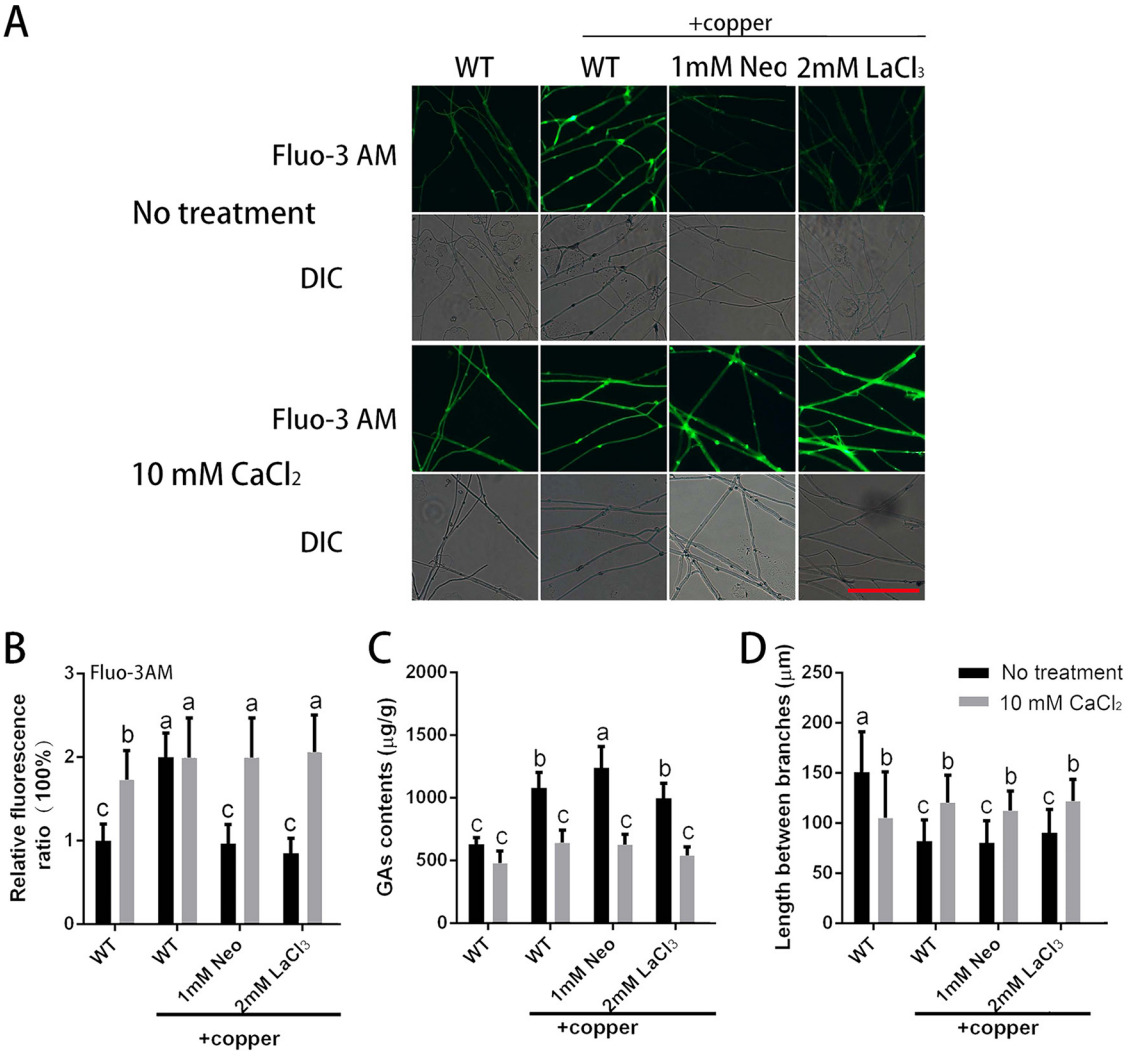

FIG 5 Exogenous Ca^{2+} application can inhibit the changes in GA content and hyphal branching induced by copper stress. (A) Changes in Ca^{2+} levels in *G. lucidum* were determined by using Fluo-3AM staining after treatment with a Ca^{2+}-related inhibitor, $CaCl_2$, or 3 mM copper. Scale bar = 100 μm. (B) Changes in the Ca^{2+} fluorescence ratio in the hyphal regions of *G. lucidum* after treatment with a Ca^{2+}-related inhibitor, $CaCl_2$ or 3 mM copper. The *y* axis represents the Ca^{2+} fluorescence ratio measured by CLSM, and the *x* axis represents the different treatments. (C) Measurement of the GA content in *G. lucidum* after treatment with a Ca^{2+}-related inhibitor, $CaCl_2$, or 3 mM copper. (D) Measurement of the hyphal branch distance in *G. lucidum* after treatment with a Ca^{2+}-related inhibitor, $CaCl_2$, or 3 mM copper. Neo (neomycin) was used as an inhibitor of phospholipase C to reduce the release of intracellular calcium stores. $LaCl_3$ was used as a blocker of calcium channels on the plasma membrane to prevent the influx of external calcium into the cytosol. The values are the mean ± SD of the results from three independent experiments. Within each set of experiments, different letters indicate significant differences between the lines ($P < 0.05$, according to a multiple-comparison one-way ANOVA).

The effects of the application of Neo (or $LaCl_3$) on the changes in the GA content and hyphal branch distance were also evaluated. Although the use of Neo (or $LaCl_3$) could suppress the increase in cytosolic Ca^{2+} content induced by treatment with 3 mM copper, the changes in GA content and hyphal branch distance were not suppressed (Fig. 5C and D). These results indicated that cytosolic Ca^{2+} is probably not directly involved in the regulation of GA biosynthesis and hyphal branching in *G. lucidum* under copper stress.

To further determine the effects of Ca^{2+}, we used exogenous 10 mM $CaCl_2$, which has no significant effect on the growth rate compared with the control group (Fig. S4A), to restore the level of intracellular Ca^{2+}. Furthermore, the independent effects of neomycin or $LaCl_3$ alone on hyphal growth, Ca^{2+} content, GA biosynthesis, and branching were also investigated (Fig. S4B to E). As shown in Fig. 5A and B, the Ca^{2+} level was significantly increased when the WT strain was treated with 10 mM $CaCl_2$

compared with the group without $CaCl_2$ treatment. In addition, the decrease in intracellular Ca^{2+} caused by Neo (or $LaCl_3$) under copper stress was significantly reduced to the level observed in the WT strain after treatment with 3 mM copper.

The GA content was also determined when the intracellular Ca^{2+} was restored by the 10 mM $CaCl_2$ treatment. As shown in Fig. 5C, the increase in the GA content induced by 3 mM copper in the WT strain was reduced by the $CaCl_2$ treatment to a level that was not significantly different from the GA content in the WT in the absence of copper treatment, and the increase in GA content due to the addition of both 3 mM copper and Neo was also significantly reduced by $CaCl_2$. RT-PCR was used to analyze the changes in the expression of key GA biosynthetic genes (*sqs*, *osc*, and *hmgr*). The upregulated expression of *sqs* and *hmgr* induced by copper was further enhanced by Neo or $LaCl_3$, as shown in Fig. S4F to H. In contrast, the upregulated expression of *sqs*, *osc*, and *hmgr* induced by 3 mM copper was reduced by $CaCl_2$ treatment, as were the expression levels of *sqs*, *osc*, and *hmgr* in mycelia treated with Neo or $LaCl_3$ under copper stress (Fig. S4). Notably, the trends in the changes of expression in these three genes and that of the GA content were completely consistent. Changes in hyphal branch distance were also observed when $CaCl_2$ was added. As shown in Fig. 5D, the hyphal branch distance in the group cotreated with 10 mM $CaCl_2$ and 3 mM copper was increased by 47% compared with the group treated with copper alone, and the distance was also increased to various degrees by 10 mM $CaCl_2$ treatment in the presence of both copper and Neo (or $LaCl_3$). These results indicated that exogenous $CaCl_2$ application could reduce the changes in the GA content and hyphal branch distance induced by copper stress.

In conclusion, the results indicate that 3 mM copper stress caused increases in the GA content with or without the use of Neo (or $LaCl_3$). However, when 10 mM Ca^{2+} was combined with the 3 mM copper treatment, the GA content was similar to those with and without the use of Neo (or $LaCl_3$). These results imply that the Ca^{2+} signal is probably not directly involved in the regulation of GA biosynthesis and hyphal branching in *G. lucidum* under copper stress.

Copper stress-induced intracellular Ca^{2+} increase occurs via ROS. Our data showed that both ROS and Ca^{2+} signaling participate in the regulation of GA biosynthesis and hyphal branching under copper stress. To analyze the relationship between the ROS and Ca^{2+} signals, we measured the level of intracellular Ca^{2+} in the WT strain when treated with DPI, Rot, AA, or H_2O_2 under copper stress. As illustrated in Fig. 6A and B, the increase in intracellular Ca^{2+} induced by 3 mM copper was significantly inhibited by DPI, Rot, or AA compared to the level of Ca^{2+} in the WT after 3 mM copper treatment alone. In addition, the inhibition of the Ca^{2+} level could be obviously enhanced when 6 mM H_2O_2 was added to restore the ROS level. These results show that the augmentation of Ca^{2+} levels induced by copper treatment was blocked when ROS overproduction was inhibited, and that restoration of the ROS level increased the Ca^{2+} level. These results suggest that the increased Ca^{2+} levels might depend on the overproduction of ROS under copper stress.

Transcriptional analysis of certain Ca^{2+} signaling-related genes was carried out in the WT strain under copper stress and treatment with DPI, Rot, AA, or H_2O_2. RT-PCR analysis showed that the upregulation of certain Ca^{2+} signaling-related genes induced by 3 mM copper was markedly inhibited by DPI, Rot, or AA treatment (Fig. 6C). However, further examination revealed that H_2O_2 promoted downregulation of the Ca^{2+} signaling-related genes. These results suggested that the copper stress-induced expression of the Ca^{2+} signaling-related genes may also be mediated by increased ROS. Thus, these findings indicated that copper-mediated activation of intracellular Ca^{2+} signaling pathways was dependent on ROS overproduction in *G. lucidum*.

The intracellular Ca^{2+} in Nox-silenced strains under copper stress was also measured. As shown in Fig. 7A and B, the 3 mM copper treatment significantly increased the intracellular Ca^{2+} levels in the WT and CK strains compared with the WT cultures not treated with copper. However, Nox silencing effectively abolished the copper-induced

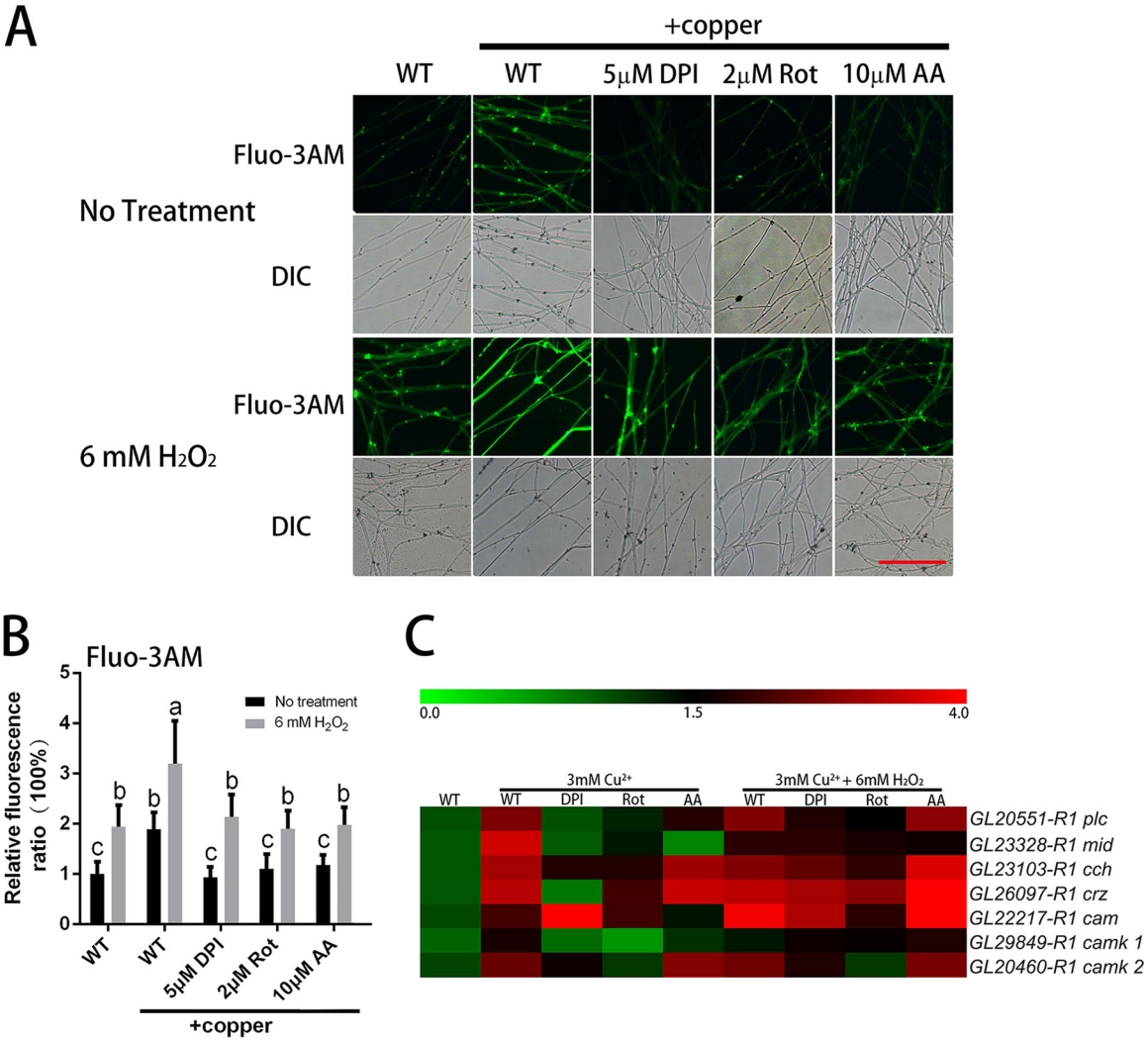

FIG 6 Copper stress induces increases in intracellular Ca^{2+} via ROS. (A) Changes in Ca^{2+} levels in *G. lucidum* were measured using Fluo-3AM staining after treatment with an ROS-related inhibitor, H_2O_2, or 3 mM copper. Scale bar = 100 μm. (B) Changes in the Ca^{2+} fluorescence ratio in the hyphal regions of *G. lucidum* after treatment with an ROS-related inhibitor, H_2O_2, or 3 mM copper. The *y* axis represents the Ca^{2+} fluorescence ratio measured by CLSM, and the *x* axis represents the different treatments. (C) The effect of ROS-related treatments on the expression of Ca^{2+}-related genes in *G. lucidum* under 3 mM copper stress. The values are the mean ± SD of the results from three independent experiments. Within each set of experiments, different letters indicate significant differences between the lines ($P < 0.05$, according to a multiple-comparison one-way ANOVA).

increases in the level of Ca^{2+}. In addition, RT-PCR analysis showed that the 3 mM copper treatment could induce the expression of certain Ca^{2+} signaling-related genes in both WT and CK (Fig. 7C and S5B), whereas the upregulation of Ca^{2+} signaling-related genes by copper was not detected in the Nox-silenced strains. These results further indicate that copper stress-induced intracellular Ca^{2+} signaling occurs via ROS.

Intracellular Ca^{2+}-regulated GA biosynthesis and hyphal branching occur via the regulation of ROS signaling under copper stress. To further assess the relationship between intracellular Ca^{2+} and ROS, the ROS level was determined when WT mycelia were treated with Neo, $LaCl_3$, or $CaCl_2$ under copper stress. As shown in Fig. 8A and B, 3 mM copper stress induced an increase in ROS, and this increase was further enhanced by 55% in the presence of 1 mM Neo and by 56% in the presence of 2 mM $LaCl_3$. These results showed that inhibiting the increases in Ca^{2+} resulted in augmented ROS production. ROS were also measured when 10 mM $CaCl_2$ was added. As shown in Fig. 8A and B, the increase in ROS under copper stress was significantly reduced by 10 mM $CaCl_2$ after both 3 mM copper treatment alone and 3 mM copper and Neo (or

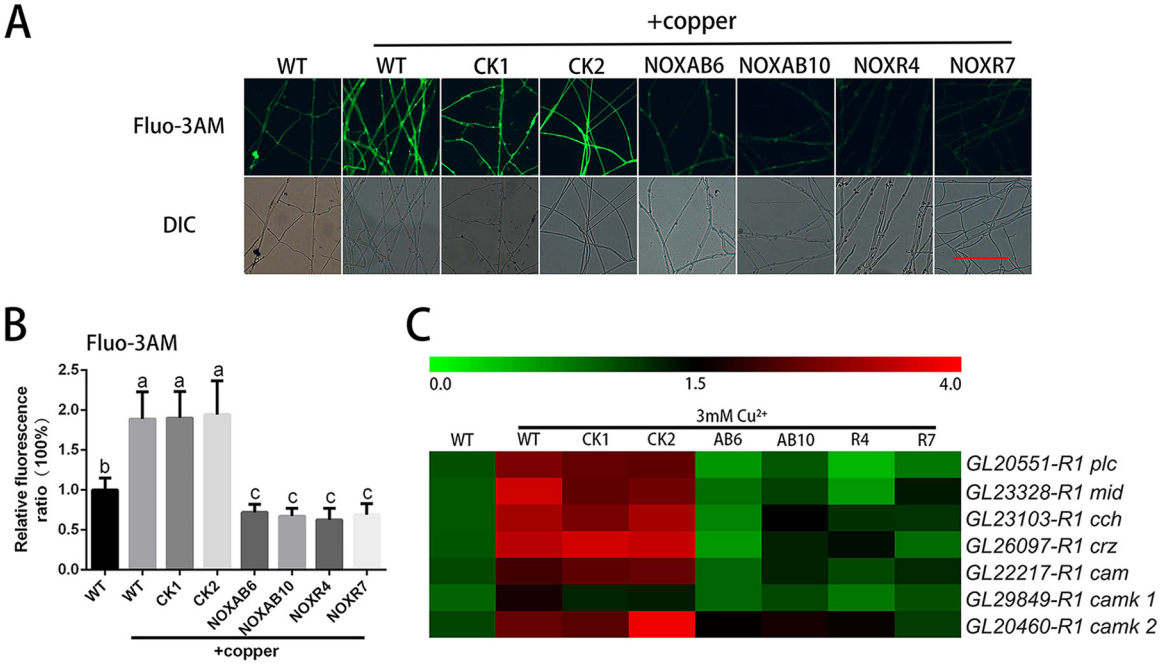

FIG 7 Copper stress-induced intracellular Ca^{2+} increase is inhibited in Nox-silenced strains. (A) Changes in Ca^{2+} levels in Nox-silenced strains were determined using Fluo-3AM staining after treatment with 3 mM copper. Scale bar = 100 μm. (B) Changes in the Ca^{2+} fluorescence ratio in the hyphal regions of Nox-silenced strains (NOXAB6 [AB6], NOXAB10 [AB10], NOXR4 [R4], and NOXR7 [R7]) after 3 mM copper treatment. The *y* axis represents the Ca^{2+} fluorescence ratio measured by CLSM, and the *x* axis represents the different strains. The values are the mean ± SD of the results from three independent experiments. Within each set of experiments, different letters indicate significant differences between the lines ($P < 0.05$, according to a multiple-comparison one-way ANOVA). (C) The effect of 3 mM copper treatment on the expression of Ca^{2+}-related genes in Nox-silenced strains.

$LaCl_3$) cotreatment. These results indicate that exogenous $CaCl_2$ treatment could effectively relieve the overproduction of ROS induced by copper stress. Furthermore, the change in the ROS levels explained the changes in GA content and hyphal branch distance when 10 mM $CaCl_2$ was added, as shown in Fig. 3C and D. These results

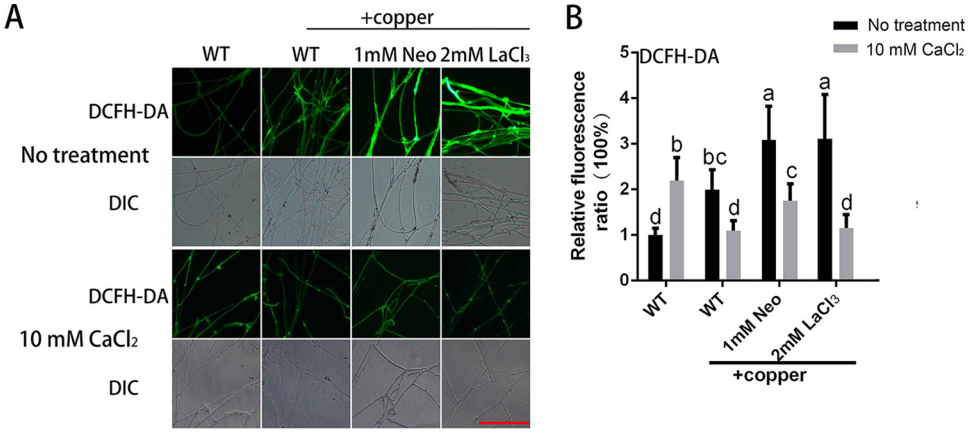

FIG 8 Intracellular Ca^{2+} regulates hyphal branching and GA biosynthesis by regulating the ROS level under copper stress. (A) Changes in the ROS levels in *G. lucidum* were determined using DCFH-DA staining after treatment with a Ca^{2+}-related inhibitor, $CaCl_2$, or 3 mM copper. Scale bar = 100 μm. (B) Changes in the ROS fluorescence ratio in the hyphal regions of *G. lucidum* after treatment with a Ca^{2+}-related inhibitor, $CaCl_2$, or 3 mM copper. The *y* axis represents the ROS fluorescence ratio measured by CLSM, and the *x* axis represents the different treatments. The values are the mean ± SD of the results from three independent experiments. Within each set of experiments, different letters indicate significant differences between the lines ($P < 0.05$, according to a multiple-comparison one-way ANOVA).

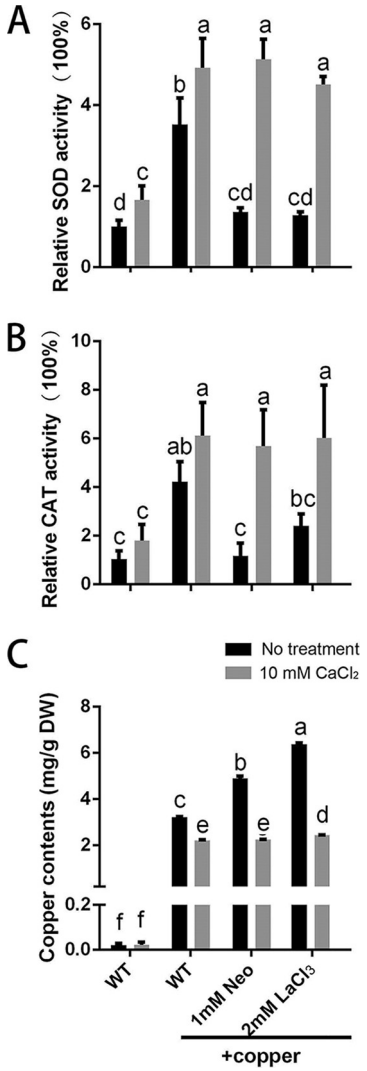

FIG 9 Intracellular Ca^{2+} regulates the ROS level by regulating antioxidase activity or the accumulation of intracellular copper. (A and B) SOD (A) and CAT (B) activity levels were measured in *G. lucidum* after treatment with a Ca^{2+}-related inhibitor, $CaCl_2$, or 3 mM copper. (C) The intracellular copper content was measured in *G. lucidum* after treatment with a Ca^{2+}-related inhibitor, $CaCl_2$, or 3 mM copper. The values are the mean ± SD of the results from three independent experiments. Within each set of experiments, different letters indicate significant differences between the lines ($P < 0.05$, according to a multiple-comparison one-way ANOVA).

indicated that the Ca^{2+}-regulated effects on GA biosynthesis and hyphal branching occur through the regulation of ROS signaling in *G. lucidum* under copper stress.

Intracellular Ca^{2+} modulates ROS levels by regulating antioxidase activity and the accumulation of intracellular copper. To investigate the mechanism by which exogenous $CaCl_2$ treatment decreased the ROS level under copper stress, the activities of certain antioxidases (superoxide dismutase [SOD] and catalase [CAT]) were assessed in *G. lucidum* mycelium under copper stress. As shown in Fig. 9A and B, the activities of SOD and CAT were significantly increased by 3 mM copper treatment to 253% and 323%, respectively. These increases in SOD activity were suppressed by 86% with 1 mM Neo and by 89% with 2 mM $LaCl_3$ and in CAT activity by 95% with 1 mM Neo and by 56% with 2 mM $LaCl_3$. The results demonstrated that the activities of certain antioxidases were significantly increased in the copper-stressed group compared with the control group. However, these copper stress-induced increases in antioxidase activities were inhibited by the Ca^{2+}-related inhibitors, which inhibited the increases in Ca^{2+} induced by copper stress (Fig. 5B). As a result, the ROS contents, which played a more

important role in regulation of copper-induced GA biosynthesis, could be kept at a high level (Fig. 8). Furthermore, the activities of SOD and CAT in the WT cultures treated with 10 mM $CaCl_2$ were also investigated and found to increase significantly with 10 mM $CaCl_2$ treatment. Specifically, cotreatment with 3 mM copper stress alone and Neo (or $LaCl_3$) resulted in similar levels of these enzymes (Fig. 9A and B). These results showed that exogenous $CaCl_2$ treatment could activate the activities of some antioxidases. Meanwhile, the ROS level was increased by 10 mM $CaCl_2$ treatment in the WT strain in the absence of copper (Fig. 8), which implied that an increase in Ca^{2+} could evoke ROS production, but at the same time, strong increases in Ca^{2+} substantially upregulated the antioxidant activities (Fig. 9A and B). These results indicated a complex regulation mechanism in the interactions between ROS and Ca^{2+} signaling transduction pathways.

Because previous studies have reported that the primary defense mechanism for heavy-metal detoxification is to reduce the intracellular content of heavy-metal ions (23), we determined the levels of intracellular copper accumulation in samples treated with 3 mM copper alone and those cotreated with Neo (or $LaCl_3$). As shown in Fig. 9C, the copper content was markedly increased to 3.31 mg/g (DW) under copper stress, and the copper content increased further by 53% at 1 mM Neo and by 99% at 2 mM $LaCl_3$ treatment. These results indicate that levels of intracellular copper accumulation were significantly increased when the increased content of Ca^{2+} under copper stress was reduced with Ca^{2+}-related inhibitors. Furthermore, the copper content in the WT strains treated with 10 mM $CaCl_2$ was investigated, and the accumulation of intracellular copper after either 3 mM copper treatment alone or 3 mM copper with Neo (or $LaCl_3$) cotreatment was significantly decreased by 10 mM $CaCl_2$ (Fig. 9C). These results show that intracellular Ca^{2+} levels participate in regulating intracellular copper accumulation.

In addition, to better investigate the role of ROS and Ca^{2+} contents in the copper stress response, the effect of the inhibitors (DPI, Rot, AA, Neo, and $LaCl_3$) on the cellular ROS and Ca^{2+} levels and the GA content in the absence of copper were also determined (Fig. S6). The results indicated that these reagents have no significant influence on GA and copper accumulation under this treatment condition.

Overall, these results suggest that exogenous $CaCl_2$ treatment could regulate the production of ROS by activating the activities of certain antioxidases and reducing the degree of intracellular copper accumulation.

DISCUSSION

During their development, fungi produce many types of secondary metabolites with important economic value. Recent studies have demonstrated that secondary metabolism is upregulated in response to environmental stress. Further studies have shown that the increased secondary metabolism induced by environmental stress depends on signaling pathways, such as the ROS and Ca^{2+} pathways. For example, Walther and Wendland found that the biosynthesis of riboflavin in *Ashbya gossypii* could be regulated by AP1 in response to ROS signaling (24). Calmodulin, which is involved in Ca^{2+} signaling, was also reported to be an important factor for aflatoxin production in *Aspergillus parasiticus* (25). However, studies to date on the signaling pathways in microorganisms have mainly focused on ascomycetes, whereas few studies in basidiomycetes have been reported, especially in larger species. Because of their unusual types of development and metabolism, it is essential to study the role of signaling in the regulation of development and metabolism in larger basidiomycetes. ROS and Ca^{2+} have also been reported to act as secondary messengers involved in signal transduction for different physiological processes. However, there are few studies on the cross talk between the ROS and Ca^{2+} signaling pathways in the regulation of development and metabolism. In the present study, we show that copper induced increases in Ca^{2+} and ROS and that there was cross talk between these intracellular signals, which led to changes in growth and secondary metabolism in *G. lucidum*.

The response to copper treatment might not be a global response to environmental stress. Copper, an important heavy-metal stressor, affects various physiological and biochemical responses, including the generation of ROS by the Fenton reaction (20). The production of GAs, which are important pharmaceutical resources, has also been reported to be significantly enhanced by copper treatment during submerged fermentation (21). Studying the mechanism by which copper regulates GA biosynthesis is helpful in understanding the mechanisms of regulation of development and metabolism in *G. lucidum*. Although environmental copper was found to accumulate in the mycelium (Fig. 9C), GAs could be isolated and purified from the mycelium without exposure to copper.

In this study, the intracellular contents of ROS and Ca^{2+} were significantly increased during the copper-induced stimulation of GA biosynthesis. To analyze whether this was a global response to heavy-metal stress or if the phenomenon was specific to copper stress alone, iron and cadmium were used to explore the changes in the GAs, ROS, and calcium levels under these conditions. The results, shown in Fig. S1, indicated that 3 mM Cd^{2+} could increase the GA, ROS, and Ca^{2+} contents compared with the WT. However, 3 mM Fe^{3+} treatment could not increase the ROS, Ca^{2+}, or GA content. These results, which were different from the changes observed in response to copper treatment, implied that the response to copper treatment might be different from the responses to iron and cadmium treatments and that the different responses caused by these ions might overlap but also differ based on their individual characteristics.

Taking these results regarding environmental stresses together, it appears that some responses to different stresses may be similar, but not all environmental stresses could induce increased GA biosynthesis via a common regulatory mechanism. These results implied that the physiological and metabolic changes in the responses of various stresses might be different.

Furthermore, as shown in Fig. 1 and 9, copper accumulated in the mycelia of *G. lucidum*. It is still unknown how copper enters the fungal cells. There is probably a copper transporter, which has not yet been identified and characterized, that plays an important role in the copper stress response, and further study of this element will be valuable.

Cytosolic ROS play an important role in the regulation of hyphal branching and secondary metabolism induced by copper stress. Hyphal branching, which increases the surface area of the colony and presumably enhances nutrient assimilation, is highly important in fungal development (26). Secondary metabolites are also important in the research and utilization of fungi based on their various types of biological activity. Accordingly, hyphal branching and secondary metabolism are thought to be important aspects of fungal growth and development. The results of the present study indicate that copper treatment could be an environmental factor that would be useful in examining the mechanisms of hyphal branching and secondary metabolism regulation. Numerous reports of increased branching have been described in fungi, such as *Neurospora crassa*, and studies of Spitzenkörper behavior suggested that branch initiation was directly related to tip growth (26, 27). For the regulatory mechanism of hyphal branching, both external and internal signaling molecules, including strigolactones and calcium, respectively, have been found to induce branching (28, 29). In a further study, Li et al. found that the deletion of the regulatory B subunits (CnB) in the calcineurin pathway resulted in a large proportion of abnormally branched germlings (30). However, the molecular processes involved in the formation and growth of hyphal branches are not clearly understood.

Our results indicated that the regulation of GA biosynthesis and hyphal branching by copper stress were dependent on ROS accumulation (Fig. 3C and D and 4C and D). These results agreed with previous reports that endogenous ROS serve as a signal that is important in the regulation of hyphal branching and GA biosynthesis (17). It has also been reported that the MeJA-induced regulation of hyphal branching and GA biosynthesis might occur via NADPH oxidase-mediated ROS signaling (13). These results showed that cytosolic ROS play a key role in the regulation of development and

metabolism in *G. lucidum* under environmental stress. Although the Fenton reaction is one of the important sources of copper stress-induced ROS generation, the mechanism by which the ROS content is increased by copper is still unknown.

Interaction between Ca^{2+} and ROS in copper treatment. We also found that copper treatment could alter the content of Ca^{2+} and that copper-induced hyphal branching and GA biosynthesis were significantly affected by exogenous Ca^{2+} (Fig. 5). This result was similar to that of Zhang et al., who reported that Ca^{2+} was a factor in the heat stress-mediated regulation of hyphal branching and GA biosynthesis (31). These results indicate that cytosolic Ca^{2+} is involved in regulating *G. lucidum* development and metabolism. However, Fig. 5B also shows that copper stress could increase the cellular level of Ca^{2+} in nontreated WT cells but not when 10 mM external Ca^{2+} was added, in which case the levels were comparable to those in non-Ca^{2+}-treated cells. This indicated that the mechanisms of Ca^{2+} release from cellular storage are involved in this regulation. Meanwhile, the two inhibitors (Neo and $LaCl_3$) showed the same profile at both concentrations, which suggested that some secondary effect might participate in this regulation. Furthermore, it appears that both cytosolic ROS and Ca^{2+} are involved in the regulation of hyphal growth and secondary metabolism in fungi. However, it remains unclear which of these two signaling pathways plays a more direct or important role, as well as the types of interaction between these two signaling pathways that are involved in the regulation of hyphal growth and secondary metabolism.

Furthermore, our results show that ROS not only regulate hyphal branching and GA content but also influence the cytosolic Ca^{2+} level under copper stress. These results were similar to those of Mu et al., who reported that ROS signaling could regulate intracellular Ca^{2+} levels (17). The findings are also consistent with the report that H_2O_2 production stimulates calcium entry into *Arabidopsis* guard cells exposed to abscisic acid by activating calcium channels located in the plasma membrane (32). Trebak et al. reported that alterations in intracellular ROS production occur through redox-based posttranslational modifications that alter the Ca^{2+} signaling networks (33). Therefore, ROS overproduction stimulates increased intracellular Ca^{2+} under copper stress in *G. lucidum*, most likely through the oxidation of groups present on these calcium channels.

Furthermore, the results indicated that cytosolic ROS regulate hyphal branching and GA biosynthesis and that cytosolic Ca^{2+} could affect these processes by regulating the cytosolic ROS. Additional research on the mechanism of regulation showed that the increase in Ca^{2+} could activate certain antioxidases and reduce the levels of cytosolic copper. Similar results were also obtained in a previous study in which the overproduction of ROS induced by cadmium toxicity was prevented by exogenous Ca^{2+} in *Pisum sativum* (34). Ca^{2+} has also been reported to reduce oxidative stress in *Lens culinaris* by modulating antioxidant enzyme activities (35). These results suggest that the increases in intracellular Ca^{2+} induced under copper stress could reduce the levels of ROS. Combining the results of this work and previous reports, there appears to be a complex relationship between the Ca^{2+} and ROS signaling pathways in the regulation of fungal development and metabolism under different environment stresses.

The ROS signaling pathway has been reported to interact with other signaling pathways in addition to Ca^{2+}. For example, Hung et al. found that NO could reduce the MeJA-induced senescence in rice leaves and that MeJA increased the ROS contents (36). He et al. found that the activation of NO production by the Gα subunits of heterotrimeric G proteins depends on H_2O_2 and that exogenously applied NO rescues the defect in UV-B-mediated stomatal closure in the *Arabidopsis thaliana* NADPH oxidase mutants AtrbohD and AtrbohF (37). These results indicate the existence of cross talk between the ROS signaling pathway and the NO signaling pathway in the regulation of stomatal closure. Furthermore, carbon monoxide treatment has also been shown to induce ROS generation in a dose-responsive manner in isolated nonsynaptic mitochondria (38). This body of research indicates that the ROS signaling pathway interacts with other signal-

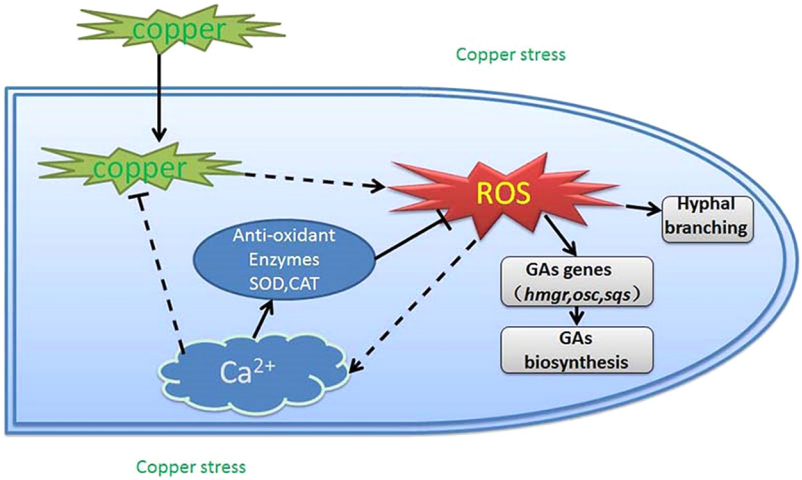

FIG 10 Schematic representation of the hypothetical model of the copper stress signaling pathway in the development and metabolism in *G. lucidum*. A model of the events that occur in hyphal cells. The intracellular copper content increases rapidly under copper stress. Intracellular copper promotes the production of ROS and leads to a burst of ROS that is required for *G. lucidum* hyphal branching and secondary metabolism. The cytosolic Ca^{2+} concentration is also increased in response to the accumulation of ROS. In addition, the increase in cytosolic Ca^{2+} concentration activates antioxidases to reduce the ROS content and intracellular copper accumulation. The black solid arrows indicate data supported by our own experiments, and the dotted arrows indicate hypothetical steps.

ing pathways; however, the cross talk among these pathways is not yet clear and requires further investigation. These findings also suggest that the mechanisms that regulate development and metabolism include a complex signaling network in plants, animals, and fungi.

Conclusion. In summary, this study provides a model of the events that occur in hyphal cells (Fig. 10). The intracellular copper content increases rapidly under copper stress. Intracellular copper promotes the production of ROS and leads to a burst in ROS that is required for *G. lucidum* hyphal branching and secondary metabolism. The cytosolic Ca^{2+} concentration is also increased in response to the accumulation of ROS. In addition, the increase in the cytosolic Ca^{2+} concentration activates antioxidases that reduce the ROS content and intracellular copper accumulation.

MATERIALS AND METHODS

Fungal strains and growth conditions. *G. lucidum* strain HG was used as a WT strain and was obtained from the culture collection of the Edible Fungi Institute, Shanghai Academy of Agricultural Science. *G. lucidum* was grown at 150 rpm for 7 days at 28°C in CYM (2% glucose, 1% maltose, 0.05% $MgSO_4 \cdot 7H_2O$, 0.2% yeast extract, 0.2% tryptone, and 0.46% KH_2PO_4) in the dark.

Copper and other chemical treatments. To evaluate the roles of intracellular ROS and Ca^{2+} under copper stress, *G. lucidum* was cultured on solid CYM for 5 days; chemical treatments were added to the solid medium on the first day. *G. lucidum* fermentation experiments were carried out in liquid medium to obtain mycelia for the production of relevant data; in this case, treatments were added at day 4 after inoculating the fermentation culture, and samples were collected at 7 days.

Various concentrations of $CuCl_2$ were added to the medium for the copper stress experiments. To test the roles of cytosolic ROS and Ca^{2+} under copper stress, the fungi were also treated with the NADPH oxidase inhibitor dibenziodolium chloride (DPI), the mitochondrial complex I inhibitor rotenone (Rot), the mitochondrial complex III inhibitor antimycin A (AA), the phospholipase C inhibitor neomycin (Neo), or the Ca^{2+} channel blocker $LaCl_3$.

Real-time PCR analysis of gene expression. Total RNA (free of DNA) was extracted from 0.1 g of fermentation mycelia using RNAiso Plus (TaKaRa, Dalian, China) and then quantified with a 5× All-In-One RT MasterMix assay kit (abm). The relative transcript levels of ROS and Ca^{2+} signal-associated proteins and GA synthesis-related proteins were determined using a quantitative real-time PCR procedure. Real-time PCR was performed using the RealPlex^2 system (Eppendorf, Germany). The PCR was conducted according to the procedure for the SYBR green real-time PCR master mix (Toyobo, Japan) supplied by the manufacturer (39). Real-time PCR-amplified fragments were determined by fluorescence using the SYBR green I dye included in the amplification kit. The gene fragments were amplified by real-time PCR using primers based on the *G. lucidum* genome sequence, as shown in Table 1 (3). The transcript levels were calculated using the standard-curve method and normalized against the 18S rRNA gene and actin gene

as the internal controls. Untreated mycelia served as the control sample against which all other genes were compared, and the expression of the control sample was defined as 1.0. The relative transcript level was analyzed using the $2^{-\Delta\Delta CT}$ method described by Livak and Schmittgen (40).

Determining hyphal branching. The distance between mycelium branches was measured as described previously (17). The *G. lucidum* strain was inoculated on glass slides covered with CYM and incubated at 28°C for 4 days. Slides carrying vegetative hyphae were incubated in the Fluorescent brightener 28 dye (2.5 μg/ml; Sigma, USA), a fluorescent dye used for the staining of fungi, to visualize the mycelium branches when the mycelium had grown onto the slides. The slides were then viewed microscopically using a Nikon Eclipse Ti-S microscope (Nikon Corporation, Japan) with a UV light. Images were recorded and processed using the NIS-Elements F package (software developed by Nikon Corporation, Japan). Hyphal branching was quantified as described by Ziv et al. (41). In the branching change analysis, the data consisted of 50 measurements of the lengths between branches and were analyzed using Fisher's least significant difference (LSD) test. In this analysis, changes in branching with a *P* value of <0.05 were considered significant.

Cytosolic ROS and Ca^{2+} labeling and detection. Cytosolic ROS and Ca^{2+} contents were measured as described previously (17). Slides carrying vegetative hyphae were incubated in the fluorescent dye 2′,7′-dichlorodihydrofluorescein diacetate (DCHF-DA; 10 mM phosphate-buffered saline [PBS] [pH 7.5]) for ROS detection or in Fluo-3 AM (10 mM PBS [pH 7.5]) to determine the free cytosolic Ca^{2+} level for 30 min at 37°C. Then, the hyphae were washed three times with 10 mM PBS (pH 7.5) to remove the excess fluorophore. The green fluorescence of the DCF- and Fluo-3 AM-labeled cells was visualized using a confocal laser scanning microscope (TCS SP2; Leica), with an emission wavelength of 488 nm produced by an argon laser and a filter of 525 to 530 nm.

The intensity of green fluorescence was quantified using the NIS-Elements F package software of the confocal microscope. To eliminate the contribution of background fluorescence, control cells without DCFH-DA or Fluo-3 AM labeling were also imaged under identical conditions. Quantification of the ROS and calcium levels was performed by selecting all region of hyphae in each photo to determine the fluorescence intensity. For each treatment, 20 images were selected for fluorescence quantification. The average fluorescence intensities of DCFH and Fluo-3 AM in the mycelia were analyzed using the ZEN lite software (Zeiss Software).

To monitor the continuous ROS and Ca^{2+} dynamics, flow cytometry was performed using a previously reported method (42). The protoplasts were prepared by a previously reported method (5) and stained with DCFH-DA or Fluo-3 AM. Measuring the fluorescence by the flow cytometry provided a measurement of the amount of dye taken up by the protoplasts and, indirectly, the amount of ROS and Ca^{2+}. To perform the flow cytometric analysis, the protoplasts were resuspended and aliquoted in liquid CYM (containing 0.6 M mannitol as an osmotic stabilizer) at 10^6 cells/ml. Then, copper was added to a final concentration of 3 mM to each individual sample, which contained 10^6 cells. Each separate sample was evaluated using an Accuri C6 Plus flow cytometer (Becton-Dickinson and Company) equipped with an air-cooled argon ion laser (488 nm, 15 mW) that was used for excitation. The collected data were analyzed with BD Accuri C6 Plus software (Becton-Dickinson). A total of 20,000 ungated events were counted.

Measurement of GAs. The GAs were extracted from fungal mycelia and measured using a previously described method (13). An Agilent 1290 infinity ultraperformance liquid chromatography (UPLC) equipped with an Agilent 1290 diode array detector and an Agilent Zorbax Eclipse plus C_{18} rapid-resolution HD 18-μm column (2.1 by 100 mm) were used to measure the GA contents. The GA content was measured using a high-performance liquid chromatography (HPLC) gradient elution method with methanol-water as the mobile phase at a constant flow rate of 0.5 ml/min. The GAs were monitored at a wavelength of 254 nm. Ganoderic acid A (Sigma, USA) was used to construct a calibration curve for the production of total GAs in the fungal mycelium. The quantification was performed according to the external calibration peak areas versus ganoderic acid A concentration graphs obtained as standards.

Enzyme activity assays. For the determination of enzyme activity, enzymes were extracted from mycelium using a previously described method (13). The protein content was determined according to the Bradford method with bovine serum albumin (BSA) as a standard.

SOD activity was assayed by monitoring the inhibition of the photochemical reduction of nitro blue tetrazolium (NBT) according to the method of Giannopolitis and Ries (43). CAT activity was assayed by measuring the rate of decomposition of H_2O_2 at 240 nm, as described by Aebi (44). Untreated mycelia served as the control sample, and the SOD or CAT activity of the control sample was defined as 1.0. The enzyme activity of other samples are displayed as the fold increase over the control sample.

Measurement of intracellular copper content. To measure the copper in the mycelia, microwave digestion generation atomic fluorescence spectrometry was performed as described for mycelia by Krakowska et al. (45). Liquid-cultivated mycelia were separated from the fermentation broth at 7 days, washed in distilled water to remove any nonspecifically bound copper, and oven-dried for 2 days at 60°C until reaching a constant weight before determination of the dry weight. The oven-dried samples were ground to a powder for analysis. The dried samples (200 mg) were digested with 8 ml of HNO_3 and 4 ml of hydrogen peroxide using microwave digestion (Milestone Ethos T). The digested sample was carefully transferred to a quartz crucible, and excess reagents were evaporated at 60°C for 45 min. Digestion of two replicates of each sample was performed. The volume of each sample was adjusted to 10 ml with doubly deionized water, and quantitative analysis of the copper in the resulting biomass was performed using the atomic absorption spectrophotometry (AAS) method by using inductively coupled plasma-optical emission spectroscopy (ICP-OES; PerkinElmer Optima 2100DV). The parameters used for the flame AAS method were as follows: type of flame/fuel, acetylene/air; wavelength, 324.8 nm; width of slit, 0.7

nm; linear range, 4.0 mg/liter; measurement time; 2 × 2 s; and curve-fitting method, linear regression. The reagent blank and analytical duplicates were used where appropriate to ensure accuracy and precision in the analysis. A range of concentrations of copper was analyzed using ICP-OES to generate a standard curve for copper.

Statistical analysis. At least three independent experiments were performed. The data were analyzed by using a multiple-comparison one-way analysis of variance (ANOVA). Within each set of experiments, different letters over the bars in Fig. 1 to 9 indicate significant differences between the lines ($P < 0.05$).

SUPPLEMENTAL MATERIAL

Supplemental material for this article may be found at https://doi.org/10.1128/AEM.00438-18.

SUPPLEMENTAL FILE 1, PDF file, 2.7 MB.

ACKNOWLEDGMENTS

This work was financially supported by the National Natural Science Foundation of China (project 31672212), the China Agriculture Research System (project CARS20), and the China Postdoctoral Science Foundation (project 2016M590468).

REFERENCES

1. Shi L, Ren A, Mu D, Zhao M. 2010. Current progress in the study on biosynthesis and regulation of ganoderic acids. Appl Microbiol Biotechnol 88:1243–1251. https://doi.org/10.1007/s00253-010-2871-1.
2. Cheng CR, Yang M, Yu K, Guan SH, Wu XH, Wu WY, Sun Y, Li C, Ding J, Guo DA. 2013. Metabolite identification of crude extract from *Ganoderma lucidum* in rats using ultra-performance liquid chromatography-quadrupole time-of-flight mass spectrometry. J Chromatogr B Analyt Technol Biomed Life Sci 941:90–99. https://doi.org/10.1016/j.jchromb.2013.10.006.
3. Chen S, Xu J, Liu C, Zhu Y, Nelson DR, Zhou S, Li C, Wang L, Guo X, Sun Y, Luo H, Li Y, Song J, Henrissat B, Levasseur A, Qian J, Li J, Luo X, Shi L, He L, Xiang L, Xu X, Niu Y, Li Q, Han MV, Yan H, Zhang J, Chen H, Lv A, Wang Z, Liu M, Schwartz DC, Sun C. 2012. Genome sequence of the model medicinal mushroom *Ganoderma lucidum*. Nat Commun 3:913. https://doi.org/10.1038/ncomms1923.
4. Mu D, Shi L, Ren A, Li M, Wu F, Jiang A, Zhao M. 2012. The development and application of a multiple gene co-silencing system using endogenous *URA3* as a reporter gene in *Ganoderma lucidum*. PLoS One 7:e43737. https://doi.org/10.1371/journal.pone.0043737.
5. Shi L, Fang X, Li M, Mu D, Ren A, Tan Q, Zhao M. 2012. Development of a simple and efficient transformation system for the basidiomycetous medicinal fungus *Ganoderma lucidum*. World J Microbiol Biotechnol 28:283–291. https://doi.org/10.1007/s11274-011-0818-z.
6. Li N, Liu XH, Zhou J, Li YX, Zhao MW. 2006. Analysis of influence of environmental conditions on ganoderic acid content in *Ganoderma lucidum* using orthogonal design. J Microbiol Biotechnol 16:1940–1946.
7. Fang QH, Zhong JJ. 2002. Effect of initial pH on production of ganoderic acid and polysaccharide by submerged fermentation of *Ganoderma lucidum*. Proc Biochem 37:769–774. https://doi.org/10.1016/S0032-9592(01)00278-3.
8. Tang YJ, Zhong JJ. 2003. Role of oxygen supply in submerged fermentation of *Ganoderma lucidum* for production of *Ganoderma* polysaccharide and ganoderic acid. Enzyme Microb Technol 32:478–484. https://doi.org/10.1016/S0141-0229(02)00338-1.
9. You BJ, Lee MH, Tien N, Lee MS, Hsieh HC, Tseng LH, Chung YL, Lee HZ. 2013. A novel approach to enhancing ganoderic acid production by *Ganoderma lucidum* using apoptosis induction. PLoS One 8:e53616. https://doi.org/10.1371/journal.pone.0053616.
10. Liang CX, Li YB, Xu JW, Wang JL, Miao XL, Tang YJ, Gu T, Zhong JJ. 2010. Enhanced biosynthetic gene expressions and production of ganoderic acids in static liquid culture of *Ganoderma lucidum* under phenobarbital induction. Appl Microbiol Biotechnol 86:1367–1374. https://doi.org/10.1007/s00253-009-2415-8.
11. Ren A, Li XB, Miao ZG, Shi L, Jaing AL, Zhao MW. 2014. Transcript and metabolite alterations increase ganoderic acid content in *Ganoderma lucidum* using acetic acid as an inducer. Biotechnol Lett 36:2529–2536. https://doi.org/10.1007/s10529-014-1636-9.
12. Ren A, Qin L, Shi L, Dong X, Mu da S, Li YX, Zhao MW. 2010. Methyl jasmonate induces ganoderic acid biosynthesis in the basidiomycetous fungus *Ganoderma lucidum*. Bioresour Technol 101:6785–6790. https://doi.org/10.1016/j.biortech.2010.03.118.
13. Shi L, Gong L, Zhang X, Ren A, Gao T, Zhao M. 2015. The regulation of methyl jasmonate on hyphal branching and GA biosynthesis in *Ganoderma lucidum* partly via ROS generated by NADPH oxidase. Fungal Genet Biol 81:201–211. https://doi.org/10.1016/j.fgb.2014.12.002.
14. Li C, Shi L, Chen D, Ren A, Gao T, Zhao M. 2015. Functional analysis of the role of glutathione peroxidase (GPx) in the ROS signaling pathway, hyphal branching and the regulation of ganoderic acid biosynthesis in *Ganoderma lucidum*. Fungal Genet Biol 82:168–180. https://doi.org/10.1016/j.fgb.2015.07.008.
15. Zhang L, Becker DF. 2015. Connecting proline metabolism and signaling pathways in plant senescence. Front Plant Sci 6:552. https://doi.org/10.3389/fpls.2015.00552.
16. Praveen Rao J, Subramanyam C. 1999. Requirement of Ca^{2+} for aflatoxin production: inhibitory effect of Ca^{2+} channel blockers on aflatoxin production by *Aspergillus parasiticus* NRRL 2999. Lett Appl Microbiol 28:85–88. https://doi.org/10.1046/j.1365-2672.1999.00460.x.
17. Mu D, Li C, Zhang X, Li X, Shi L, Ren A, Zhao M. 2014. Functions of the nicotinamide adenine dinucleotide phosphate oxidase family in *Ganoderma lucidum*: an essential role in ganoderic acid biosynthesis regulation, hyphal branching, fruiting body development, and oxidative-stress resistance. Environ Microbiol 16:1709–1728. https://doi.org/10.1111/1462-2920.12326.
18. Xu YN, Zhong JJ. 2012. Impacts of calcium signal transduction on the fermentation production of antitumor ganoderic acids by medicinal mushroom *Ganoderma lucidum*. Biotechnol Adv 30:1301–1308. https://doi.org/10.1016/j.biotechadv.2011.10.001.
19. González A, Cabrera Mde L, Henriquez MJ, Contreras RA, Morales B, Moenne A. 2012. Cross talk among calcium, hydrogen peroxide, and nitric oxide and activation of gene expression involving calmodulins and calcium-dependent protein kinases in *Ulva compressa* exposed to copper excess. Plant Physiol 158:1451–1462. https://doi.org/10.1104/pp.111.191759.
20. Nakajima H, Hara K, Yamamoto Y, Itoh K. 2015. Effects of Cu on the content of chlorophylls and secondary metabolites in the Cu-hyperaccumulator lichen *Stereocaulon japonicum*. Ecotoxicol Environ Saf 113:477–482. https://doi.org/10.1016/j.ecoenv.2014.12.038.
21. Tang YJ, Zhu LW. 2010. Improvement of ganoderic acid and *Ganoderma* polysaccharide biosynthesis by *Ganoderma lucidum* fermentation under the inducement of Cu^{2+}. Biotechnol Prog 26:417–423.
22. Lang RJ, Hashitani H, Tonta MA, Suzuki H, Parkington HC. 2007. Role of Ca^{2+} entry and Ca^{2+} stores in atypical smooth muscle cell autorhythmicity in the mouse renal pelvis. Br J Pharmacol 152:1248–1259. https://doi.org/10.1038/sj.bjp.0707535.
23. Shahid M, Pourrut B, Dumat C, Nadeem M, Aslam M, Pinelli E. 2014.

Heavy-metal-induced reactive oxygen species: phytotoxicity and physicochemical changes in plants. Rev Environ Contam Toxicol 232:1–44.
24. Walther A, Wendland J. 2012. Yap1-dependent oxidative stress response provides a link to riboflavin production in *Ashbya gossypii*. Fungal Genet Biol 49:697–707. https://doi.org/10.1016/j.fgb.2012.06.006.
25. Rao JP, Subramanyam C. 2000. Calmodulin mediated activation of acetyl-CoA carboxylase during aflatoxin production by *Aspergillus parasiticus*. Lett Appl Microbiol 30:277–281. https://doi.org/10.1046/j.1472-765x.2000.00717.x.
26. Harris SD. 2008. Branching of fungal hyphae: regulation, mechanisms and comparison with other branching systems. Mycologia 100:823–832. https://doi.org/10.3852/08-177.
27. Martínez-Núñez L, Riquelme M. 2015. Role of BGT-1 and BGT-2, two predicted GPI-anchored glycoside hydrolases/glycosyltransferases, in cell wall remodeling in *Neurospora crassa*. Fungal Genet Biol 85:58–70. https://doi.org/10.1016/j.fgb.2015.11.001.
28. Dor E, Joel D, Kapulnik Y, Koltai H, Hershenhorn J. 2011. The synthetic strigolactone GR24 influences the growth pattern of phytopathogenic fungi. Planta 234:419–427. https://doi.org/10.1007/s00425-011-1452-6.
29. Makhzoum A, Yousefzadi M, Malik S, Gantet P, Tremouillaux-Guiller J. 2017. Strigolactone biology: genes, functional genomics, epigenetics and applications. Crit Rev Biotechnol 37:151–162. https://doi.org/10.3109/07388551.2015.1121967.
30. Li F, Wang ZL, Zhang LB, Ying SH, Feng MG. 2015. The role of three calcineurin subunits and a related transcription factor (Crz1) in conidiation, multistress tolerance and virulence in *Beauveria bassiana*. Appl Microbiol Biotechnol 99:827–840. https://doi.org/10.1007/s00253-014-6124-6.
31. Zhang X, Ren A, Li MJ, Cao PF, Chen TX, Zhang G, Shi L, Jiang AL, Zhao MW. 2016. Heat stress modulates mycelium growth, HSP expression, ganoderic acid biosynthesis and hyphal branching of *Ganoderma lucidum* via cytosolic Ca^{2+}. Appl Environ Microbiol 82:4112–4125. https://doi.org/10.1128/AEM.01036-16.
32. Pei ZM, Murata Y, Benning G, Thomine S, Klusener B, Allen GJ, Grill E, Schroeder JI. 2000. Calcium channels activated by hydrogen peroxide mediate abscisic acid signalling in guard cells. Nature 406:731–734. https://doi.org/10.1038/35021067.
33. Trebak M, Ginnan R, Singer HA, Jourd'heuil D. 2010. Interplay between calcium and reactive oxygen/nitrogen species: an essential paradigm for vascular smooth muscle signaling. Antioxid Redox Signal 12:657–674. https://doi.org/10.1089/ars.2009.2842.
34. Rodríguez-Serrano M, Romero-Puertas MC, Pazmino DM, Testillano PS, Risueno MC, Del Rio LA, Sandalio LM. 2009. Cellular response of pea plants to cadmium toxicity: cross talk between reactive oxygen species, nitric oxide, and calcium. Plant Physiol 150:229–243. https://doi.org/10.1104/pp.108.131524.
35. Talukdar D. 2012. Exogenous calcium alleviates the impact of cadmium-induced oxidative stress in *Lens culinaris* medic. Seedlings through modulation of antioxidant enzyme activities. J Crop Sci Biotechnol 15:325–334.
36. Hung KT, Kao CH. 2004. Nitric oxide acts as an antioxidant and delays methyl jasmonate-induced senescence of rice leaves. J Plant Physiol 161:43–52. https://doi.org/10.1078/0176-1617-01178.
37. He JM, Ma XG, Zhang Y, Sun TF, Xu FF, Chen YP, Liu X, Yue M. 2013. Role and interrelationship of Gα protein, hydrogen peroxide, and nitric oxide in ultraviolet B-induced stomatal closure in *Arabidopsis* leaves. Plant Physiol 161:1570–1583. https://doi.org/10.1104/pp.112.211623.
38. Queiroga CSF, Almeida AS, Martel C, Brenner C, Alves PM, Vieira HLA. 2010. Glutathionylation of adenine nucleotide translocase induced by carbon monoxide prevents mitochondrial membrane permeabilization and apoptosis. J Biol Chem 285:17077–17088. https://doi.org/10.1074/jbc.M109.065052.
39. Shi L, Qin L, Xu Y, Ren A, Fang X, Mu D, Tan Q, Zhao M. 2012. Molecular cloning, characterization, and function analysis of a mevalonate pyrophosphate decarboxylase gene from *Ganoderma lucidum*. Mol Biol Rep 39:6149–6159. https://doi.org/10.1007/s11033-011-1431-9.
40. Livak KJ, Schmittgen TD. 2001. Analysis of relative gene expression data using real-time quantitative PCR and the $2^{-\Delta\Delta CT}$ method. Methods 25:402–408. https://doi.org/10.1006/meth.2001.1262.
41. Ziv C, Feldman D, Aharoni-Kats L, Chen S, Liu Y, Yarden O. 2013. The N-terminal region of the *Neurospora* NDR kinase COT1 regulates morphology via its interactions with MOB2A/B. Mol Microbiol 90:383–399. https://doi.org/10.1111/mmi.12371.
42. Cui C, Zhang Y, Han H, Zhang S. 2012. Improvement of FISH-FCM enumeration performance in filamentous yeast species in activated sludge by snailase partial digestion. Yeast 29:111–117. https://doi.org/10.1002/yea.2894.
43. Giannopolitis CN, Ries SK. 1977. Superoxide dismutases: I. Occurrence in higher plants. Plant Physiol 59:309–314.
44. Aebi H. 1984. Catalase *in vitro*. Methods Enzymol 105:121–126. https://doi.org/10.1016/S0076-6879(84)05016-3.
45. Krakowska A, Reczynski W, Muszynska B. 2016. Optimization of the liquid culture medium composition to obtain the mycelium of *Agaricus bisporus* rich in essential minerals. Biol Trace Elem Res 173:231–240. https://doi.org/10.1007/s12011-016-0638-y.